Front. Med. 2020, 14(3): 335–356
https://doi.org/10.1007/s11684-019-0705-9

RESEARCH ARTICLE

Chinmedomics facilitated quality-marker discovery of Sijunzi decoction to treat spleen qi deficiency syndrome

Qiqi Zhao[1], Xin Gao[1], Guangli Yan[1], Aihua Zhang[1], Hui Sun[1], Ying Han[1], Wenxiu Li[1], Liang Liu[2], Xijun Wang (✉)[1,2,3]

[1]National Chinmedomics Research Center, Sino-America Chinmedomics Technology Collaboration Center, National TCM Key Laboratory of Serum Pharmacochemistry, Laboratory of Metabolomics, Department of Pharmaceutical Analysis, Heilongjiang University of Chinese Medicine, Harbin 150040, China; [2]State Key Laboratory of Quality Research in Chinese Medicine, Macau University of Science and Technology, Avenida Wai Long, Taipa, Macau, China; [3]National Engineering Laboratory for the Development of Southwestern Endangered Medicinal Materials, Guangxi Botanical Garden of Medicinal Plant, Nanning 530023, China

Abstract **Sijunzi decoction (SJZD) is a Chinese classical formula to treat spleen qi deficiency syndrome (SQDS) and has been widely used for thousands of years. However, the quality control (QC) standards of SJZD are insufficient. Chinmedomics has been designed to discover and verify bioactive compounds of a variety of formula rapidly. In this study, we used Chinmedomics to evaluate the SJZD's efficacy against SQDS to discover the potential quality-markers (q-markers) for QC. A total of 56 compounds in SJZD were characterized *in vitro*, and 23 compounds were discovered *in vivo*. A total of 58 biomarkers were related to SQDS, and SJZD can adjust a large proportion of marker metabolites to normal level and then regulate the metabolic profile to the health status. A total of 10 constituents were absorbed as effective ingredients that were associated with overall efficacy. We preliminarily determined malonyl-ginsenoside Rb2 and ginsenoside Ro as the q-markers of ginseng; dehydrotumulosic acid and dihydroxy lanostene-triene-21-acid as the q-markers of poria; glycyrrhizic acid, isoglabrolide, and glycyrrhetnic acid as the q-markers of licorice; and 2-atractylenolide as the q-marker of macrocephala. According to the discovery of the SJZD q-markers, we can establish the quality standard that is related to efficacy.**

Keywords traditional Chinese medicine; Sijunzi decoction; spleen qi deficiency syndrome; Chinmedomics; quality-marker

Introduction

Traditional Chinese medicine (TCM) attaches importance to the unity and integrity of the human body itself and its relationship with nature. TCM holds that the human body is a holistic organism [1], which considers the five Zang organs as the center and the whole body tissues and organs linked to each other through the meridian and collateral system and finally completes the unified functional activities of the body through the functions of essence, qi, blood, and body fluid. As the most basic substance of the human body, qi possesses the function of promotion, warm, defense, and domination. Qi also comes from the congenital essence of parents before birth and is converted from daily diet and natural air, which we breathed in through the lung. Qi deficiency is a common clinical syndrome and generally manifested by pale complexion, breath shortness, limb weakness, dizziness, sweating, and low voice [2,3]. In clinical practice, spleen qi deficiency syndrome (SQDS) generally shows two kinds of pathological changes; one is the weakening of the spleen transport function, and the other is the insufficient generation of blood that is transferred from qi. Symptoms, such as anorexia, abdominal distention, loose stools, and fatigue are the main manifestations. Other symptoms include common diarrhea, epigastric pain, abdominal pain, edema, asthma, flaccidity syndrome, children's chancre, Western medicine chronic gastroenteritis, chronic nephritis, chronic bronchitis, and bronchial asthma. The distinguished points of SQDS compared with qi deficiency syndrome can be summarized as yellowish face, decreased food consumption, loose stool, slow pulse, and pale tongue with whitish coating.

Sijunzi decoction (SJZD), which was first reported 940 years ago in "*TaipingHuiminHejiJufang*," is a common

Received November 14, 2018; accepted June 25, 2019
Correspondence: Xijun Wang, xijunwangls@126.com

prescription for SQDS [4] in TCM. This prescription is made up of Radix Ginseng (*Panax ginseng* C. A. Meyer), macrocephala (*Atractylodes macrocephala* Koidz.), poria (*Poria cocos* [Schw.] Wolf.), and licorice (*Glycyrrhiza uralensis* Fisch.). The prescription is beneficial to the spleen and can enhance qi movement. As a superior drug, ginseng can replenish spleen qi, thereby strengthening the spleen and removing dampness as an important formula ingredient. Macrocephala and ginseng support each other, thereby strengthening the spleen and make the formula efficacy strongstronger. With the spleen characteristics, such as drying, poria, which can be considered as an assistant of ginseng, can enhance the spleen function and dry the needless moisture in the human body. Licorice blended with various medicinal herbs can enhance the potency of ginseng and macrocephala. Given that these four kinds of Chinese herbal medicines are mild in nature, this prescription is also called "Four gentlemen decoction."

As the most basic method of treating disease in TCM, the effectiveness of prescription is crucial. The quality of Chinese medicine is the guarantee of clinical efficacy [5], and it is also a most critical factor in the development of Chinese medicine industry. At present, the research level of Chinese medicine quality is gradually increasing [6–8], but this condition still cannot meet the increasing quality control (QC) requirements. In particular, the research on the effective material basis of TCM is weak [9], thereby leading to poor correlation between the QC indices of TCMs and their effectiveness [10]. At the same time, the QC specificity is poor, and the standard of various medicinal materials is often evaluated by the same index. Meanwhile, the single index component is difficult to complete the quality attribute of the complex system in TCM. To improve the quality and QC of Chinese medicine products, researchers introduced the concept of quality-marker (q-marker for the characteristics of the medical system of Chinese medicine, which mainly includes the medicine biological properties, medicine manufacturing process, and medicine compatibility theory). Syndromes and prescriptions are two basic problems of TCM [11], and the prescriptions are formed under the guidance of compatibility principles. Understanding the value of TCM clinical experience and whether and why a prescription is effective are the first problems to be solved [12,13]. Chinmedomics is a biological language to describe the TCM efficacy scientifically. Efficacy evaluation can be completed based on biomarkers, which reflected the TCM syndrome and the efficacy of TCM formulae [16,17] by the ingenious integration of serum pharmacochemistry and omics technology [14,15], thereby finally illustrating the scientific value of TCM [18]. The method of Chinmedomics is closely related to the correlation degree of the effectiveness of "TCM-effective constituents q-markers." Thus, the idea and practice of discovering the q-markers of TCM can be achieved.

Materials and method

Materials and reagents

All medicines formulating SJZD (i.e., *P. ginseng*, *A. macrocephala*, *P. cocos*, and *G. uralensis*) were purchased from Harbin TongRenTang Drug Store (Harbin, China) and identified by Professor Aihua Zhang of the National Chinmedomics Research Center. Reagents, such as acetonitrile, methanol, distilled water, formic acid, and leucine enkephalin, used for ultraperformance liquid chromatography/mass spectrometry (UPLC/MS) analysis were all of high-performance LC (HPLC) grade. The other reagents were of analytical grade.

Folium senna extract and SJZD sample preparation

The literature *Treatise on the Spleen and Stomach* written by Dongyuan Li indicated that "the medicine of bitter cold damages the spleen and stomach most." In our experiment, we used bitter cold and diarrhea-coupled disordered dietary methods to replicate the SQDS model. A total of 400 g Senna were added into 4000 mL of boiling water with soaking for 10 min and filtrated. Then, the filtrate was concentrated under the condition of rotary evaporation at 50 °C, and the concentrate was cooled to room temperature and subsequently made it into freeze-dried powder. The powder yield was 21.02% and stored at ambient temperature in the dryer. We took an appropriate amount of freeze-dried powder and dissolved it in distilled water of 0.2 g/mL including crude 20% Senna before use.

The SJZD samples were prepared by water extraction and obeyed to the original decocting method recorded in *TaipingHuiminHejiJufang*. First, the crude drugs of SJZD were ground to powder state at the proportion of 3:3:3:2, soaked in water at room temperature for 1 h (1:8, w/v), and boiled for 1 h and then 0.5 h. We collected the filtrate through a 16-slice gauze and then concentrated the filtrates and dried to powder by using vacuum freeze-drying technology. The powder yield was 29.57%. We stored the powder at ambient temperature in the dryer and took an appropriate amount of freeze-dried powder and dissolved it in distilled water with the amount of 1 g/mL SJZD before use.

Animals with spleen qi deficiency and drug administration

A total of 50 specific pathogen free (SPF) grade male Sprague–Dawley rats (9-week-old) were commercially supplied by the Experimental Animal Center of Harbin Medical University. These rats were maintained at room temperature 24 ± 2 °C with a preset 12 h light/dark cycle and allowed free access to water and food pellets. The rats were allowed to undertake 7 days to adapt to the

environment and kept in metabolism cages for 3 days of acclimatization before the formal experiment. We randomly divided all rats into five groups, including two control groups (CON ($n = 10$), control ($n = 10$)), two model groups (MOD ($n = 10$), model ($n = 10$) and one SJZD group ($n = 10$)). The SJZD group would receive equal dose of human body of SJZD for 7 days. Model rats (20 rats) were successively orally administered with 20% Senna extract (4 g/(kg·day)) for 7 days. During this period, on single days (1st, 3rd, 5th, and 7th day), the model group was kept hollow, and those in the double days were overfed. As a contrast, the control groups were given equal amount of distilled water daily with standard diet. During treatment, the SJZD group was orally administered with SJZD (equivalent to 0.5625 g/(kg·day) body weight of crude drug of SJZD). The corresponding control groups and the model groups were gavaged equal volume of distilled water under the same condition.

Biological sample collection and preparation

During model and drug efficacy evaluation, the blood samples of the control, model, and SJZD groups were collected from the hepatic portal vein after anesthetized with pentobarbital sodium. Viscera were sampled for subsequent organ index and histopathology study. After centrifugation at 3500 rpm for 15 min at 4 °C, the serum samples were transferred into clean tubes and stored in liquid nitrogen for serum biochemical parameter analysis, metabolomic study, and serum pharmacochemistry analysis. Particularly, the SJZD group was collected in the same way at 1 h after having orally administered with SJZD. The rats were placed into the corresponding metabolism cage for a continuous duration of 12 h, and the urine samples were transferred for − 80 °C storage after being scrupulously centrifuged. A mixed sample containing aliquots of all the collected serum samples and urine samples was sampled as the QCs, which were crucial for optimization during metabolomic analytical method development.

Model evaluation and SJZD efficacy

Rat general status

The rat general status, including the body weight, food intake, fecal state (diarrhea, anal contamination, and defecation after pulling the tail), hair color, lethargy, fatigue, and many other exhibitions, was observed throughout the experiment. Different symptoms and bodily representation were among different groups. The symptoms of model rats' weight loss and anorexia can be regarded as the clinical SQDS patients' manifestation of poor appetite, less eating and reduced weight. Rats' loose stools and soft stools can be used to characterize diarrhea in patients with SQDS. As the same phenotypes of patients with SQDS that easily tired and are weak, the rats can have decreased activity, hunch their backs forward, squint the eyes, and flock together. The SQDS can even dull the shine and tone of the rat hair.

Thymus and spleen indices

The spleen controlling digestion and the dysfunction of this organ can lead to immune dysfunction of the body. The commonly used indices to observe the changes in immune system are the thymus and spleen indices [19]. Thus, we observed the abnormal immune function in model rats by monitoring the spleen and thymus indices. In our experiment, 3% pentobarbital Na was injected into the rats' abdominal cavity according to the body weights (0.2 mL per 100 g body weight). Then, the rat's thymus and spleen were quickly removed. The viscera were subsequently dried with a filter paper, and the thymus and spleen were weighed. Then, the visceral indices were calculated as follows:

Thymus index = thymus mass / body mass,
Spleen index = spleen mass / body mass.

Plasma biochemical parameters and histopathological analyses

To evaluate the replicating success of the SQDS rat model, we analyzed the biochemical indices, such as plasma amylase level, serum D-xylose absorption level, gastrin (GAS) level, and motilin (MOT) level. The stomach and small intestine tissues were stained with hematoxylin and eosin and observed by light microscopy. Image analysis was carried out using Image-Pro Plus 5.0 software.

Determination of gastric food remnant and propulsive rates of small intestine in rats

Fasting was carried out on the first night of rat handling, and semisolid rice paste, which contained black active carbon, was taken by gavage before 30 min of anesthetization (1 mL per 100 g body weight). The stomach was ligated between the gastric cardia and pylorus and then removed and dried with a filter paper. Then, the stomach body was cut along the large stomach bend. Subsequently, the stomach contents were washed, dried again, and then weighed to obtain the stomach net weight. The difference between the total and net stomach weight was the quality of gastric food remnant. At the same time, we rapidly removed the small intestine, stripped it from the mesentery, and spread it on a white paper. We also measured the distance between the pyloric to ileocecal portion and the distance between the pyloric to the black semisolid rice

paste. The ratio of pyloric to black semisolid paste and the total length of pyloric to ileocecal area were the rate of small intestine propulsion.

The gastric food remnant rate and small intestine propulsion rate were calculated as follows:

$$\text{Gastric food remnant rate } (\%) = [(T-N)/S] \times 100\%,$$

where T is the stomach total weight, N is the stomach net weight, and S is the semisolid rice paste weight taken by the rat.

$$\text{Small intestine propulsion rate } (\%) = [(I-P)/I] \times 100\%,$$

where P is the black semisolid rice paste pushing distance, and I is the small intestine full length.

Metabolomics study

Sample preparation

To avoid the interference of high molecular proteins, we carried out one-step protein precipitation by mixing 200 μL of serum with 800 μL of methanol. After vigorous mixing and centrifugation at low temperature, the serum supernatant was transferred for the following dryness under vacuum in a SpeedVac concentrator. Before formal analysis, 100 μL of methanol was added to dissolve each dried residue, and the redissolved sample was added into an autosampler vial and then injected into the UPLC/MS system to acquire the full scan chromatograms. Urine samples were prepared by mixing urine with equal volume of distilled water and adding the resulting solution to each vial and then waited for UPLC/MS system analysis. Serum and urine QCs were dissolved or diluted in the same manner, which can provide a representative analysis for the instrument stability monitoring.

UPLC-Q-TOF conditions

Synapt High Definition-Q-Tof Mass Spectrometer and Waters Acquity™ UPLC system (Waters Corp., Milford, MA, USA) were used for the mass spectrometry detection and the chromatographic separation of the serum and urine samples. An aliquot of 2 μL of sample solution was injected into an ACQUITY UPLC BEH C18 column (50 mm × 2.1 mm, 1.7 μm; Waters Corporation, Milford, USA) or an ACQUITY UPLC™ HSS T3 column (100 mm × 2.1 mm i.d., 1.8 μm; Waters Corporation, Milford, USA) at 45 °C. The flow rate was 0.4 mL/min. The optimal mobile phase consisted of a linear gradient system of (1) 0.1% formic acid in acetonitrile and (2) 0.1% formic acid in water. The detailed linear gradients of serum and urine analyses are listed in Tables S1 and S2, and the optimal conditions for MS analysis are listed in Table S3. Needle wash cycle was conducted to remove the remnants between every two sample injections, and a lock mass of leucine enkephalin was used via a lock spray interface in positive and negative ion modes to ensure accuracy during MS analysis.

Data analysis

The metabolomics method coupled with pattern recognition had been performed reproducibly and precisely in our previous publications [20,21]. UPLC-Q-TOF/MS data for the serum and urine samples were imported to the Progenesis-QI manager (Waters Corp.) for an automatic pre-processing. All data were normalized to the summed total ion intensity per chromatogram, and the resultant data matrices were imported into the EZinfo 2.0 software for principal component analysis (PCA) and orthogonal partial least-squared discriminant analysis (OPLS-DA). MassFragment™ application manager (Waters Corp., Milford, USA) was used to characterize the MS/MS fragment ion analysis process. The reconstruction, interaction, and pathway analysis of potential biomarkers were performed with MetPA software on the basis of the Metlin, HMDB, and Chemispider databases to analyze biomarkers and identify the metabolic pathways. SPSS 18.0 for Windows was used to analyze the metabolomics data statistically. Statistically significant differences with $P \leqslant 0.05$ in mean values were significant and performed by 2-tailed, 2-sample Student's *t*-test or 1-way ANOVA and Bonferroni multiple comparisons, which were post-tested as appropriate.

Serum pharmacochemistry analysis

SJZD constituent analysis

A total of 200 mg SJZD freeze-dried powder were critically weighed, and 50% methanol was added to the scale of 10 mL bottle and then weighed again. The samples underwent 30 min ultrasonic process, cooled to room temperature, and weighed again. Methanol (50%) was added to add weight. This 20 mg/mL solution was mixed again and filtered through the 0.22 μm filter membrane. The continuous filtrate was collected for the following UPLC/MS analysis. We used Synapt High Definition Q-Tof Mass Spectrometer with 5 μL of samples injected into Waters Acquity™ UPLC system (Waters Corp., Milford, MA, USA) to analyze and characterize the chemical components of SJZD. The structure of the chemical components can be characterized by retention time, and the MS/MS information in high and low energy data can be utilized for further component identification.

Serum sample preparation

The serum samples of the model and the SJZD-dosed groups were used for the serum pharmacochemistry analysis. The optimal conditions for sample preparation are as follows: 40 μL of phosphoric acid was first added into 2 mL of serum samples, and these samples were applied onto preactived OASIS® hydrophile–lipophile balance solid-phase extraction (SPE) column after a careful ultrasonication and vortexing operation. Then, the SPE column was eluted with 4 mL of 100% methanol, and the eluent was dehydrated by N gas at 37 °C. The residue was redissolved in 200 μL of 100% methanol and centrifuged at 13 000 rpm for 15 min at 4 °C. A total of 5 μL of the supernatant were injected for UPLC-MS analysis.

UHPLC-Q-TOF conditions

To analyze the compounds existing in the SJZD and serum after the oral administration of SJZD, the SJZD and serum sample constituent analyses had the same UHPLC-Q-TOF condition. Chromatographic separation was performed on Waters Acquity™ UPLC system (Waters Corp., Milford, MA, USA) equipped with an ACQUITY UPLC BEH C18 column (50 mm × 2.1 mm, 1.7 μm; Waters Corporation, Milford, USA). The column was maintained at 45 °C, and the optimal mobile phase was consisted of a linear gradient system of (A) 0.1% formic acid in acetonitrile and (B) 0.1% formic acid in water, as follows: 0–3.0 min, 5%–30% A; 3.0–4.0 min, 30%–34% A; 4.0–5.0 min, 34%–34.5% A; 5.0–8.0 min, 34.5%–40% A; 8.0–9.0 min, 40%–50% A; 9.0–10.0 min, 50%–75% A; 10.0–12.0 min, 75%–85% A; and 12.0–13.0 min, 85%–99% A. The flow rate was set at 0.4 mL/min, and during analysis, all samples were kept at 4 °C to reduce maximized degradation. The optimal conditions for MS analysis, including the source temperature, desolvation gas temperature, cone gas flow, desolvation gas flow, and capillary voltage, were screened. The data acquisition rate was set to 0.2 s/scan, with 0.1 s inter scan delay. Data were collected in a centroid mode from 50 Da to 1500 Da.

SJZD constituent analysis in vivo

Tentative prototype components, which were absorbed into rat organisms, were analyzed by the imported MS data of the dosed and model serum samples to the MarkerLynx software. The EZinfo 2.0 software was also applied to characterize the potential discriminated variables by PCA. We consider substance a tentative prototype component only when ion peaks are present in dosed chromatogram and absent in the model chromatogram. These conditions tentatively suggested that the components were compared with the MS and MS/MS data with full scan analysis of the chemical compounds of the SJZD sample *in vitro* and further analyzed with the module of elemental composition tool and MS/MS fragment mass spectra. Considering the metabolites of orally administrated drugs, which are transformed in gut microflora, liver, and phase II detoxifying enzymes into active metabolites, we also screened the potential metabolite products by the Metaboanalyst Software (Waters Corporation, Milford, MA, USA). This software can realize an automatic screening with a potential biotransformation lists, such as oxidation, reduction, hydrolysis, glucuronide, sulfation, methylation, and acetylation. Other analysis parameters, including MS trace retention time range, mass defect filter, retention time window, control peak area ratio, and absolute area, were all set in the response threshold window.

Correlation analysis between marker metabolites and absorbed constituents by using Chinmedomics strategy

Chinmedomics strategy was efficiently utilized to discover active compounds, which may contribute to the main therapeutic effect of SJZD in SQDS treatment. A correlation model between the metabolic biomarkers and chemical compound was established. Thus, high correlation compounds with relevant parameters of $0.65 < |r| < 1$ or $0.55 < |r| < 0.65$ can be recognized. This result indicated extremely high correlation and high correlation, respectively. The organic combination of "*TCM syndrome biomarkers – direct acting substances in vivo – drug effect biomarkers*" and the analysis methods of the two groups of variables (plotting of correlation between marker metabolites and serum constituents, PCMS) in an organism suggested a new angle in evaluating the biological efficacy of the prescriptions, thereby laying the foundation for the study of q-markers.

Results

Rat general status and visceral index

In the SQDS model replication stage of our experiment, we seriously recorded the rats' general status every day. With a similar body weight before model replication, the weight of the CON group in the model replicating process increased steadily and rapidly, while the growth of MOD rats was slow. The body mass of these two groups of rats began to show statistically significant difference ($P < 0.05$) on the 3rd day, and extremely significant difference appeared from the 5th day during model replicating process ($P < 0.01$, Fig. 1A). We also discovered that in the whole stage, the rats in the CON group had a strong body with smooth hair, and their activity was flexible and did not release loose stools. Meanwhile, the MOD rats showed a completely different state. From the 2nd day of the model replication, the MOD rats began to

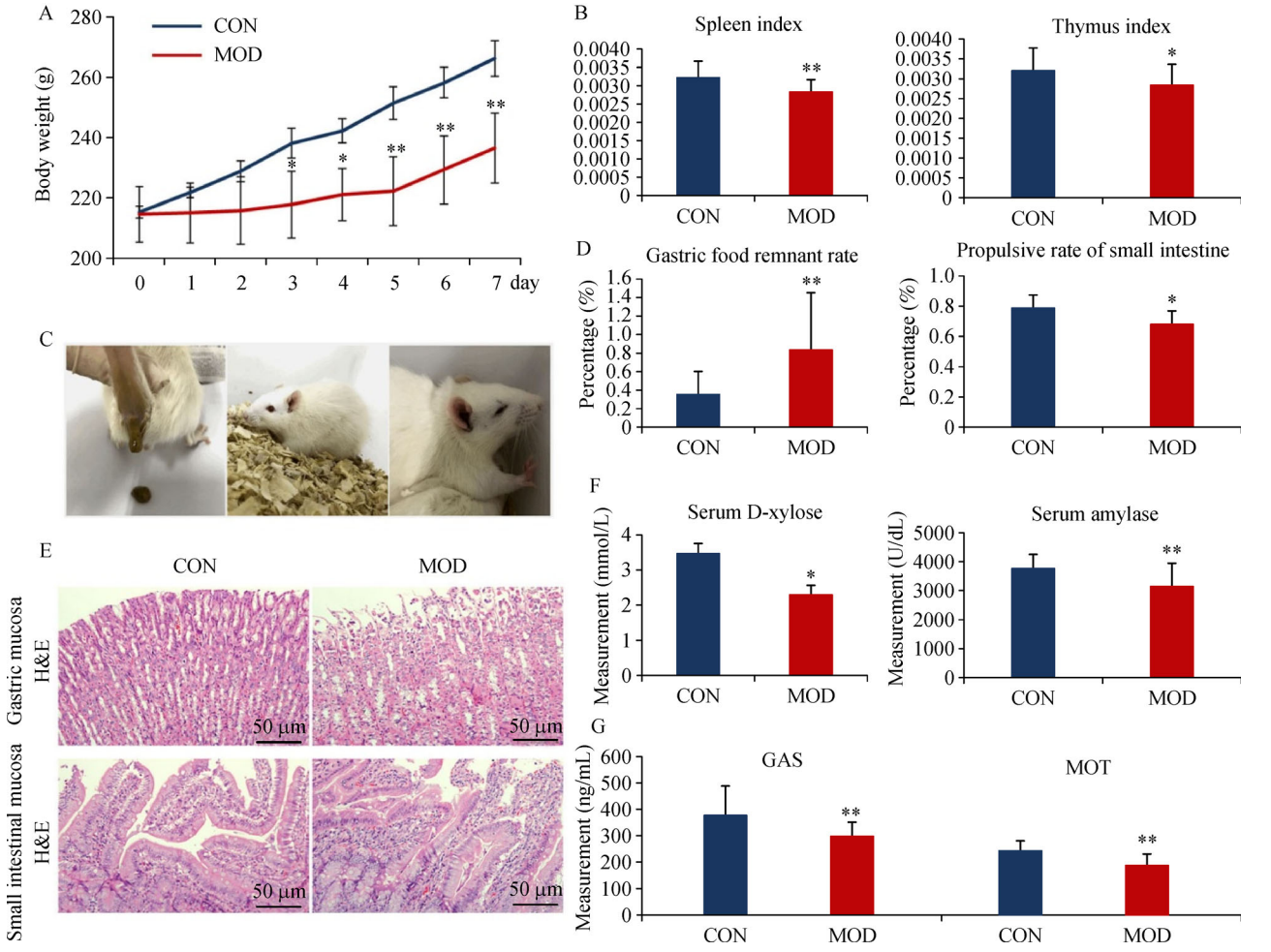

Fig. 1 Model evaluation of spleen qi deficiency syndrome. (A) Body weight between the CON and MOD groups. (B) Spleen and thymus indices between the CON and MOD groups. (C) General state of model rats during model replication period. (D) Gastric food remnant and small intestine propulsive rates between the CON and MOD groups. (E) Gastric and small intestinal mucosa from the MOD group showed disorderly epithelial cells, unclearly muscular layer, slight erosion and exudation. (F) Serum D-xylose level and amylase level between CON and MOD groups. (G) GAS and MOT level between CON and MOD groups. *$P < 0.05$ and **$P < 0.01$ compared with the CON group.

release loose stools and are languid and lazy. The stool was unformed and accompanied by mucus. On the third day, obvious squinting eyes, hunching backs, and flocking together were observed. On the 5th day, the MOD rat hair withered and showed hair fall, with anus covered with feces. On the 7th day of the model replication, the rats' ears and tails displayed bleached color with lags in response and even apathetic to resist capture. Diarrhea and anorexia in MOD rats continued throughout the 7 days, and few rats developed blood stool during the modeling process (Fig. 1C). After 7 days of therapy with SJZD, the body weight of the therapy group and the SQDS model group showed a significant upward trend, but the weight growth of the untreated model group was slower than that of the SJZD group (Fig. 2A). The stool status of the rats that were orally administrated with SJZD gradually tended to be normal. On the 4th day of therapy, the rats in each group had no dilute excretion, and the activity increased significantly with the increase in fighting and chasing. At the same time, as a comparison for SJZD therapy, all general status of the model group rats without SJZD oral administration had a slower recovery than the therapy group. The decrease of immune function is an important aspect of deficiency of spleen qi. After 7-day model replication, the spleen index and thymus index were monitored in this experiment to determine if the immune function was abnormal. As shown in Fig. 1B, the spleen index of SQDS MOD rats displayed extremely significant difference with those in the CON group ($P < 0.01$), and the thymus index showed significant difference ($P < 0.05$). This result demonstrated that the immune function of the MOD group rats may be abnormal. After 7 days of SJZD therapy, we compared the spleen and thymus index again, but the difference between the model and SJZD group was statistically insignificant despite a certain callback (Fig. 2B).

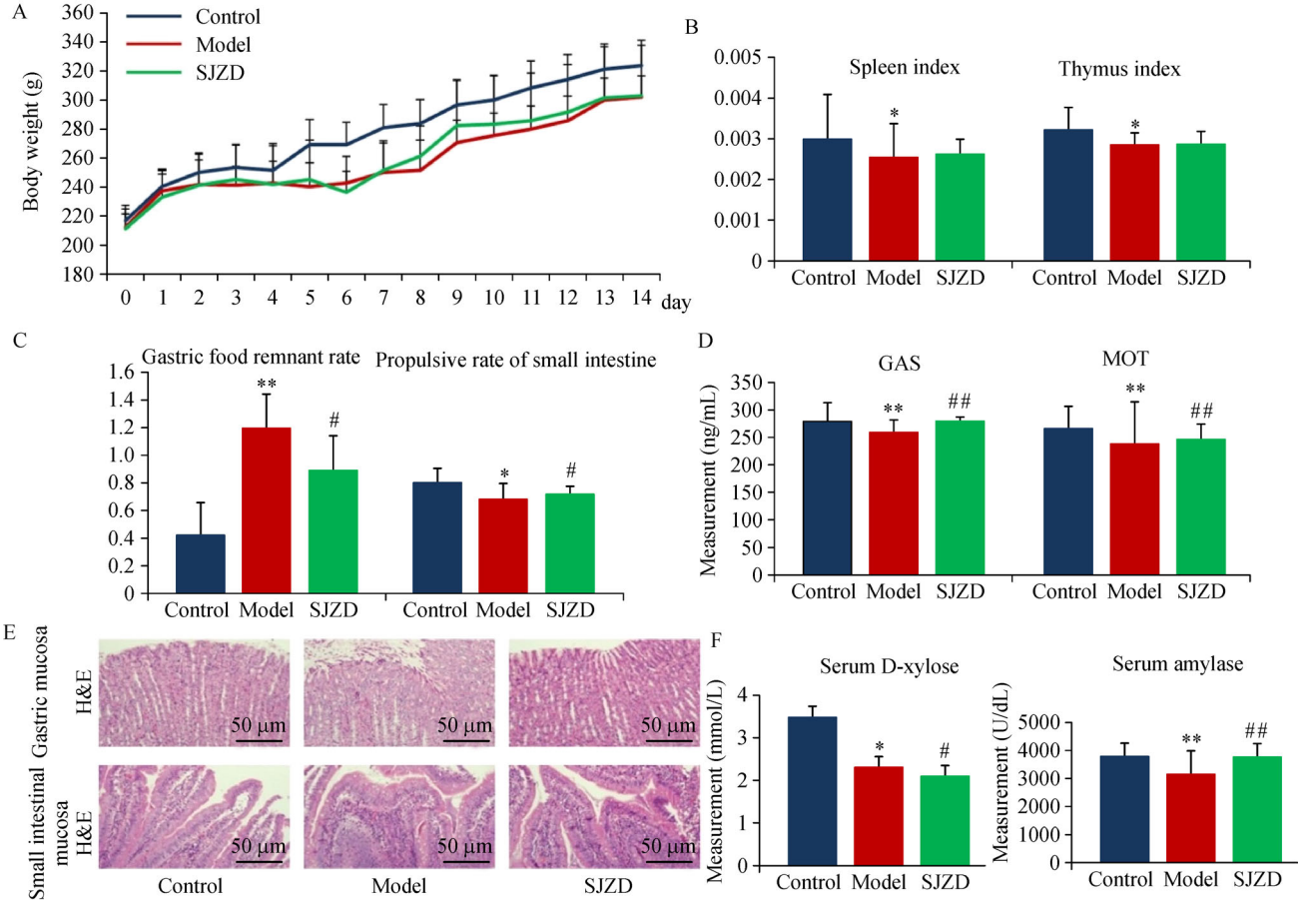

Fig. 2 SJZD efficacy evaluation on spleen qi deficiency syndrome. (A) Body weight of the control, model, and SJZD groups. (B) Spleen and thymus indices of the control, model, and SJZD groups. (C) Gastric food remnant and small intestine propulsive rates of the control, model, and SJZD groups. (D) GAS and MOT level of the control, model, and SJZD groups. (E) Gastric and small intestinal mucosa from the SJZD group showed improved epithelial cells and tissue lesion. (F) Serum D-xylose level, amylase level, GAS, and MOT level of the control, model, and SJZD groups. $^{*}P < 0.05$ and $^{**}P < 0.01$ compared with the control group; $^{\#}P < 0.05$ and $^{\#\#}P < 0.01$ compared with the model group.

Gastric food remnant rate and propulsive rate of small intestine

The stomach is a primary digestive organ for food [22], and the small intestine is a structural unit to absorbing nutrients after food is initially decomposed [23,24]. Under the same time condition, rapid gastric food emptying indicates strong initial digestion [25]. The propelling distance of the decomposed food in the small intestine within a unit time reacts to the ability to absorb nutrients through the small intestinal mucosal epithelial cells. During our experiment, the rat stomach and small intestinal tissues were removed and observed by the naked eye first. Most gastric tissues of the rats were pale pink, smooth, and soft with regular mucosal folds, while slight whitening and hardened symptoms can be observed in a few SQDS MOD rats. In terms of small intestinal morphology, rich blood filling in the mesentery can be observed in CON rats, and the small intestinal peristalsis was evident with pink bowel wall. However, in several modeling rats, the elasticity of the intestinal was poor, the color of the intestinal wall was gray, and the intestinal peristalsis showed significant decrease. After the peptic organ was dried with filter paper and generally weighed, the remnant rate of stomach food and the experimental results of the small intestine propulsion were analyzed (Fig. 1D). The amount of residual food in the stomach of model rats was extremely significantly higher ($P < 0.01$) than that in the CON group. This result indicated that the digestive function of the MOD rat was weakened. The small intestine of the SQDS MOD rat was also found abnormal with the propelling rate slower than that in the CON group, with statistically significant difference between the two groups ($P < 0.05$). After SJZD therapy, although the intestinal wall adhered occasionally, the peristalsis of the small intestine tended to increase compared with the model group, and the stomach color became pale red; no abnormality was found. In the analysis of gastric food remnant and small intestine propulsive rates (Fig. 2C), the stomach digestion and small intestine propulsion abilities were promoted in rats treated by SJZD and significantly higher than those in the model group, with a certain

difference between the model and control groups ($P < 0.05$).

Biochemical analysis and histopathological observations

After the oral administration of Senna and irregularly fed for 7 days, the rats in the MOD groups showed evident fatigue, diarrhea, and retardation. GAS is one of the main hormones in the gastrointestinal hormone family with the closest relationship to the spleen; it has many physiologic functions, such as stimulating gastric acid secretion and promoting the proliferation of gastrointestinal mucosa [26]. Spleen weakness, loss of appetite, reduced contents in the stomach, and digestion of protein breakdown products all reduced GAS secretion [27]. MOT is secreted mainly in the Mo cells, peptiderma neuron in the duodenum, the proximal end of jejunum mucous hidden fossa, and the peptiderma neurons in intestinal nerve clusters. MOT can cause the contraction of smooth muscle through the specific receptors acting on the smooth muscle cells, promote gastrointestinal movement, and improve contractility and tension of the gastrointestinal tract [28]. The activity of serum amylase is a sensitive and specific detection index reflecting the function of digestion and absorption. Inadequate secretion is bound to affect the food digestion and nutrient absorption. Amylase determination is an objective indicator to SQDS diagnosis. D-xylose is almost nonexistent in the blood with the cause of intestinal mucosa absorption in the proximal intestine and immediately excreted by the kidneys; the intestinal mucosa absorption can be assessed by measuring the xylose content in the blood or urine after a certain interval of oral xylose [29]. In our analysis, the serum samples of the rats were tested for the serum amylase levels, serum D-xylose, serum GAS, and serum MOT. The results are shown in Fig. 1F and 1G. Compared with the CON groups, the serum level of amylase, D-xylose, GAS, and MOT all abnormally decreased. These findings indicated that the rat model showed evident digestion and absorption disorder, which were the characteristics of SQDS. After treatment, the serum level of amylase, GAS, and MOT showed extremely significant upward trend compared with the model group ($P < 0.01$, Fig. 2D), and the serum D-xylose level revealed a significant unregulated trend ($P < 0.05$, Fig. 2F). As an essential diagnostic method, the histopathological examination of the stomach and small intestine was performed [30]. No signs of apparent abnormality were observed in the CON group. However, in MOD group, the epithelial cells in the gastric mucosa of the rats were shed and incomplete, which was accompanied by slight erosion and mucous exudation. The small intestinal mucosa showed defects, the structure of the muscular layer was unclear, and the nuclear distribution was scattered with number reduced (Fig. 1E). Treatment with SJZD improved the tissue lesion to a certain degree (Fig. 2E).

Representative biomarkers for SQDS and effects of SJZD on the basis of metabolite profile

Using the optimal chromatography-mass spectrometry method, we obtained the serum and urine electrospray ionization mass spectrometry metabolite profiling data (Figs. S1 and S2). In urine metabolomics study, the urine metabolic profile of the MOD group is moving away from the CON direction during the model replication, also showing the success of model replication from a metabolic perspective (Fig. 3B). Under the help of experimental data mathematical models, such as PCA and OPLS-DA (Fig. 3A and 3C), we roughly obtained 156 and 289 alternative chemical compounds in the serum and urine, which fit to the principle of *P*-value less than 0.05 and VIP of more than 1. Through a further screening with databases, such as human metabolome database, kyoto encyclopedia of genes and genomes database, Melin, Chemispider, and a MS/MS fragment matching (Fig. 4), we tentatively screened out 21 biomarkers in rat serum, which could stand for SQDS, and 37 biomarkers were tentatively screened out in rat urine. The detailed information of these serum and urine metabolites is, respectively, illustrated in Tables 1 and 2. The biomarkers relative measurements before and after SJZD treatment are represented in Fig. 5. For further evaluation of the drug efficacy, the metabolite profile after orally administrated SJZD was obtained. In addition, we could clearly found through the pictures that with the SJZD therapy, urine and serum metabolite profiles all gathered to control (Fig. 6A and 6B). MetabAnalyst 4.0 and KEGG websites were further utilized to explore the metabolites' relative disordered pathway. The results are shown in Fig. 6C and 6D. To help clearly understand the disordered state from the metabolic perspective, we reconstructed the pathway, which involved several key markers, which we tentatively identified in our serum and urine metabolic analysis (Fig. 7).

Identification of constituents *in vitro* and the compounds absorbed into blood

UPLC-MSMS and Masslynx software were used to analyze and characterize the chemical compounds of SJZD. The structure of the chemical components can be characterized by retention time, and MS/MS information under the collision energy could be provided. Through the manual operation of peak picking and fragment matching, we finally characterized 56 chemical components of SJZD *in vitro*, consisting of 20 compounds in ginseng, 4 compounds in macrocephala, 15 compounds in poria,

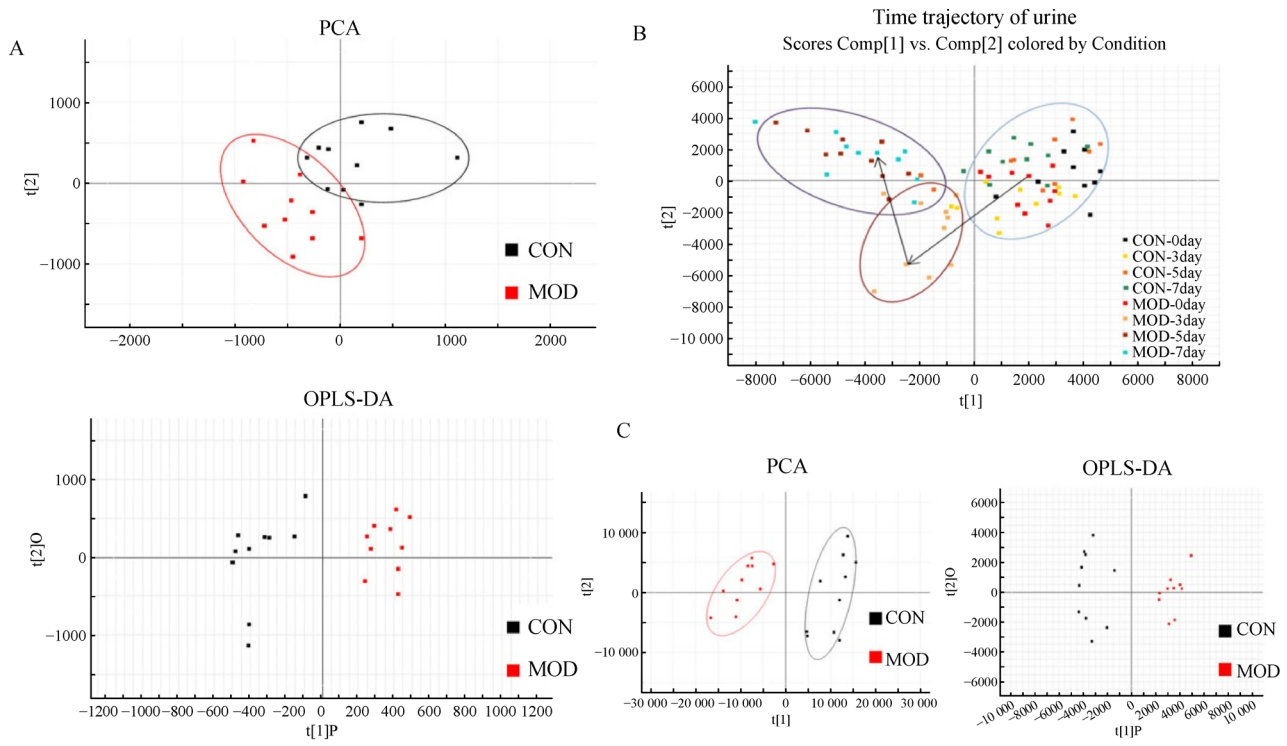

Fig. 3 Multivariate analysis in SQDS serum and urine metabolomics study. (A) PCA score plot (above) and OPLS-DA score plot (below) between different groups in serum metabolomics study. (B) Time trajectory of rat urine during the model replication. (C) PCA score plot (left) and OPLS-DA score plot (right) between different groups in urine metabolomics study.

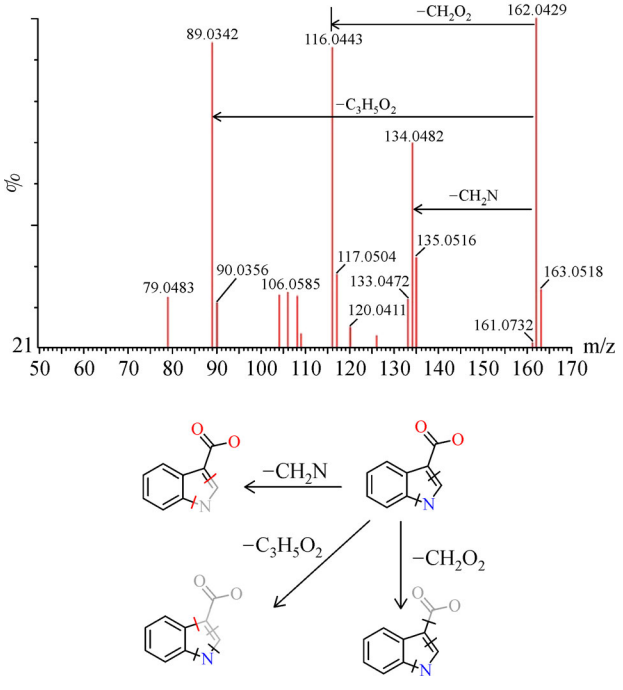

Fig. 4 Chemical structure and the mass fragment information of indole-3-carboxylic acid, identified as the SQDS rat urine biomarker in positive ion mode. The precise molecular mass and the fragments were detected by a mass spectrometer (UPLC-Q-TOF-MS) and determined within a reasonable degree of measurement error (< 5 mDa).

and 17 compounds in licorice. The detailed information of these compounds is illustrated in Table S4. For the identification of constituents *in vitro*, global profiles in the positive and negative were analyzed, and we screened the absorbed compounds with the methods of multiple pattern recognition. The ES-BPI chromatograms of the SJZD sample, model sample, and dosed sample acquired by UPLC-MS are shown in Fig. 8A. With the PCA method, we compare the differences of serum chromatograms between the dosed group and the model group (Fig. 8B), and only the compounds responded in the dosed group did we regard as potentially absorbed compounds (Fig. 8C). Finally, 18 prototypical chemical compound peaks were tentatively characterized *in vitro* by the use of serum pharmacochemistry. The detailed information of these compounds is illustrated in Table S5. The ES-BPI chromatogram marked with characterized compounds after oral SJZD is illustrated in Fig. 9. With regard to the result of metabolized chemical compound, in the composition analysis of Radix Ginseng and macrocephala, they were found entering the blood in prototype form, with no metabolites detected. We found that poria metabolites, such as tumulosic acid and dehydrofulvic acid, the licorice metabolites, such as 18β-glycyrrhetic acid, liquiritin-7-O-glucuronide, and formononetin 7-O-β-D-glucuronide in rats' serum, and the detailed information of these compounds are illustrated in Table S6.

Table 1 Detailed information of biomarkers tentatively identified by serum metabolomics

No.	Rt	M/Z determined	M/Z calculated	Adducts	Actual_M	Proposed composition	Postulated identity	Trend
1	1.08	136	136	M + Na	113.05	$C_5H_7NO_2$	1-Pyrroline-2-carboxylic acid	↓
2	1.09	154	154.1	M + H	153.04	$C_7H_7NO_3$	3-Hydroxyanthranilic acid	↓
3	1.68	157.1	157.1	M + Na	134.07	$C_4H_{10}N_2O_3$	L-Canaline	↓
4	2.19	201	201	M − H	202.03	$C_{11}H_6O_4$	Bergaptol	↑
5	2.54	514.3	514.3	M − H	515.29	$C_{26}H_{45}NO_7S$	Taurocholic acid	↑
6	2.81	448.3	448.3	M − H	449.31	$C_{26}H_{43}NO_5$	Chenodeoxyglycocholic acid	↓
7	3.6	315.2	315.2	M − H	316.2	$C20H_{28}O_3$	4-Hydroxyretinoic acid	↓
8	3.64	282.3	282.3	M + H	281.27	$C_{18}H_{35}NO$	Oleamide	↑
9	3.91	333.2	333.2	M − H	334.21	$C_{20}H_{30}O_4$	Prostaglandin A2	↓
10	3.91	289.2	289.2	M + H	288.21	$C_{19}H_{28}O_2$	Testosterone	↓
11	3.93	518.3	518.3	M + H	517.32	$C_{26}H_{48}NO_7P$	LysoPC(18:3(9Z,12Z,15Z))	↑
12	4.31	303.2	303.2	M − H	304.24	$C_{20}H_{32}O_2$	Arachidonic acid	↓
13	4.84	255.2	255.2	M − H	256.24	$C_{16}H_{32}O_2$	Palmitic acid	↓
14	4.9	1092	1092	M + H	1090.7	$C_{56}H_{102}N_2O_{18}$	Ganglioside GA2 (d18:1/9Z-18:1)	↑
15	5.01	295.2	295.2	M − H	296.24	$C_{18}H_{32}O_3$	9,10-Epoxyoctadecenoic acid	↓
16	6.19	552.4	552.4	M + H	551.4	$C_{28}H_{58}NO_7P$	LysoPC(20:0)	↑
17	6.73	780.6	780.6	M + Na	757.56	$C_{42}H_{80}NO_8P$	PC(18:1(11Z)/16:1(9Z))	↑
18	7.02	253.2	253.2	M − H	254.22	$C_{16}H_{30}O_2$	Palmitoleic acid	↓
19	7.13	742.5	742.5	M − H	743.55	$C_{41}H_{78}NO_8P$	PC(15:0/18:2(9Z,12Z))	↑
20	7.28	578.4	578.4	M + H	577.41	$C_{30}H_{60}NO_7P$	LysoPC(22:1(13Z))	↑
21	7.42	808.6	808.6	M + H	807.58	$C_{46}H_{82}NO_8P$	PC(20:2(11Z,14Z))	↑

The arrows in the table show relative change trends of potential biomarkers compared with the model group. ↑ indicates over expressed; ↓ indicates insufficiently expressed.

Correlation analysis between marker metabolites and absorbed constituents

Under the premise that SJZD could effectively improve the abnormal index of SQDS rats in our experiment, we utilized the Chinmedomics strategy and established a correlation between marker metabolites and serum constituents (PCMS) to screen the effective substances in SJZD acting against SQDS. During this analysis, correlation coefficient (r) between the serum constituents and serum/urine metabolites was calculated by Pearson's correlation analysis method, and we could obtain which serum constituents were the most related to therapeutic effect. As shown in Figs. 10 and 11, the degrees of correlation are shown in different color heat maps. For further screening, we proposed that the components in the serum have to be at least one extreme correlation with the metabolites, which could be considered as the most related to the drug effects and strict in urine correlation. On the basis of at least one extreme correlation with the urine metabolites, the drug components absorbed into serum need to be highly/extremely correlated with one or more other metabolites, which could be considered as the most related to the drug effects. With the screen principles mentioned previously, we selected seven compounds, namely, liquirtin, malonyl-ginsenoside Rb2, ginsenoside Ro, glycyrrhetnic acid, 2-atractylenolide, dehydrotumulosic acid, and isoglabrolide, as the tentatively effectual components in serum compounds-serum metabolite correlation analysis and eight compounds, namely, formononetin, malonyl-ginsenoside Rb2, ginsenoside Ro, glycyrrhizic acid, glycyrrhetnic acid, 2-atractylenolide, isoglabrolide, and dihydroxy lanostene-triene-21-acid, as the tentatively effectual components in serum compounds-urine metabolite correlation analysis.

Q-markers in SJZD

Under the guidance of Chinmedomics, we preliminarily characterized the closest correlation compounds, which have curative biological activity in SQDS rat serum/urine metabolomics as the alternative q-marker for SJZD. They are liquirtin, formononetin, malonyl-ginsenoside Rb2, ginsenoside Ro, glycyrrhetnic acid, glycyrrhizic acid, 2-atractylenolide, dehydrotumulosic acid, and isoglabrolide. To determine whether a compound can be really regarded as a q-marker, to conform to the principle of further screening is necessary. This process is the essential conditions for q-marker that the compound must be the inherent secondary metabolite in the TCM and TCM

Table 2 Detailed information of biomarkers tentatively identified by urine metabolomics

No.	Rt	M/Z determined	M/Z calculated	Adducts_H +	Adducts_H −	Actual_M	Proposed composition	Postulated identity	Trend
1	0.68	195.0504	195.0505	–	195.051	196.0583	$C_6H_{12}O_7$	Galactonic acid	↓
2	0.71	114.0661	114.0672	114.067	–	113.0589	$C_4H_7N_3O$	Creatinine	↑
3	0.76	300.0389	300.0389	–	300.039	301.0468	$C_8H_{15}NO_9S$	N-Acetylglucosamine 6-sulfate	↓
4	0.77	203.1508	203.1511	203.15	–	202.143	$C_8H_{18}N_4O_2$	Dimethyl-L-arginine	↓
5	0.79	335.0955	339.0961	335.096	–	334.0907	$C_{17}H_{19}C_lN_2OS$	Chlorpromazine-N-oxide	↓
6	0.8	243.0973	243.0971	243.098	–	242.0903	$C_{10}H_{14}N_2O_5$	Thymidine	↓
7	0.84	149.0451	149.0445	–	149.044	150.0528	$C_5H_{10}O_5$	β-D-ribopyranose	↑
8	0.89	70.0651	70.0655	70.0654	–	69.0578	C_4H_7N	1-Pyrroline	↑
9	0.89	132.0665	132.067	132.066	–	131.0582	$C_5H_9NO_3$	4-Hydroxy-L-proline	↑
10	0.9	191.0186	191.0191	–	191.019	192.027	$C_6H_8O_7$	Citric acid	↓
11	0.9	173.0079	173.0083	–	173.008	174.0164	$C_6H_6O_6$	Trans-aconitic acid	↓
12	1.21	121.065	121.0653	121.065	–	120.0575	C_8H_8O	Phenylacetaldehyde	↑
13	1.21	138.0915	138.0911	138.092	–	137.0841	$C_8H_{11}NO$	Tyramine	↑
14	1.29	111.0086	111.0081	–	111.008	112.016	$C_5H_4O_3$	2-Furoic acid	↓
15	1.29	173.0075	173.0081	–	173.008	174.0164	$C_6H_6O_6$	Dehydroascorbic acid	↓
16	1.69	238.0935	238.0929	238.094	–	237.0862	$C_9H_{11}N_5O_3$	Dyspropterin	↑
17	1.95	136.0753 /134.0591	136.0745 /134.0589	136.076	134.06	135.0684	C_8H_9NO	N-Acetylarylamine	↓
18	2.5	208.0969	208.0971	208.097	–	207.0895	$C_{11}H_{13}NO_3$	N-Acetyl-L-phenylalanine	↑
19	2.74	220.1183	220.118	220.118	–	219.112	$C_{10}H_{13}N_5O$	Cis-zeatin	↑
20	2.85	279.1335	279.1336	279.134	–	278.1267	$C_{14}H_{18}N_2O_4$	N1-(α-D-ribosyl)-5, 6-dimethyl-benzimidazole	↓
21	2.94	216.9804	216.981	–	216.981	217.9885	$C_7H_6O_6S$	5-Sulfosalicylic acid	↑
22	3.02	162.0561 /160.0392	162.0555 /160.0399	162.055	160.039	161.0477	$C_9H_7NO_2$	Indole-3-carboxylic acid	↓
23	3.23	167.0335	167.0338	–	167.034	168.0423	$C_8H_8O_4$	Homogentisic acid	↑
24	3.41	206.0448 /204.0295	206.0455 /204.0289	206.045	204.029	205.0375	$C_{10}H_7NO_4$	Xanthurenic acid	↓
25	3.74	190.0449	190.0512	190.05	–	189.0426	$C_{10}H_7NO_3$	Kynurenic acid	↓
26	3.95	208.0607	208.0612	208.061	–	207.0532	$C_{10}H_9NO_4$	4-(2-Aminophenyl)-2, 4-dioxobutanoic acid	↓
27	4.27	178.0492	178.0495	–	178.05	179.0582	$C_9H_9NO_3$	Hippuric acid	↓
28	4.57	164.0722 /162.0558	164.071 /162.0561	164.071	162.055	163.0633	$C_9H_9NO_2$	3-Methyldioxyindole	↓
29	4.57	340.1041 /338.0881	340.1042 /338.0882	340.104	338.088	339.0954	$C_{15}H_{17}NO_8$	6-Hydroxy-5-methoxyindole glucuronide	↓
30	4.8	192.0658	192.0661	–	192.066	193.0739	$C_{10}H_{11}NO_3$	Phenylacetylglycine	↓
31	5.18	229.143	229.1433	–	229.143	230.1518	$C_{12}H_{22}O_4$	Dodecanedioic acid	↓
32	5.37	173.0813	173.0809	–	173.081	174.0892	$C_8H_{14}O_4$	Suberic acid	↓
33	6.15	255.0671 /253.0514	255.0665 /253.0504	255.066	253.05	254.0573	$C_7H_{14}N_2O_6S$	5-L-Glutamyl-taurine	↑
34	6.23	297.0975	297.0983	–	297.098	298.1053	$C_{14}H_{18}O_7$	2-Phenylethanol glucuronide	↓
35	6.23	175.0241	175.0235	–	175.024	176.0321	$C_6H_8O_6$	D-Glucurono-6,3-lactone	↓
36	7.2	181.0862	181.086	181.086	–	180.0786	$C_{10}H_{12}O_3$	Coniferyl alcohol	↑
37	8.48	407.2785	407.2793	–	407.279	408.2876	$C_{24}H_{40}O_5$	Cholic acid	↑

The arrows in the table show relative change trends of potential biomarkers compared with the model group. ↑ indicates over expressed; ↓ indicates insufficiently expressed.

products, or the chemical substance formed during preparation. The substance should also be a chemical substance derived from the certain only medicinal herb instead of other medicinal herbs, thereby needing a clear chemical structure and biological activity and can be identified and quantified. Lastly, the compound selection is

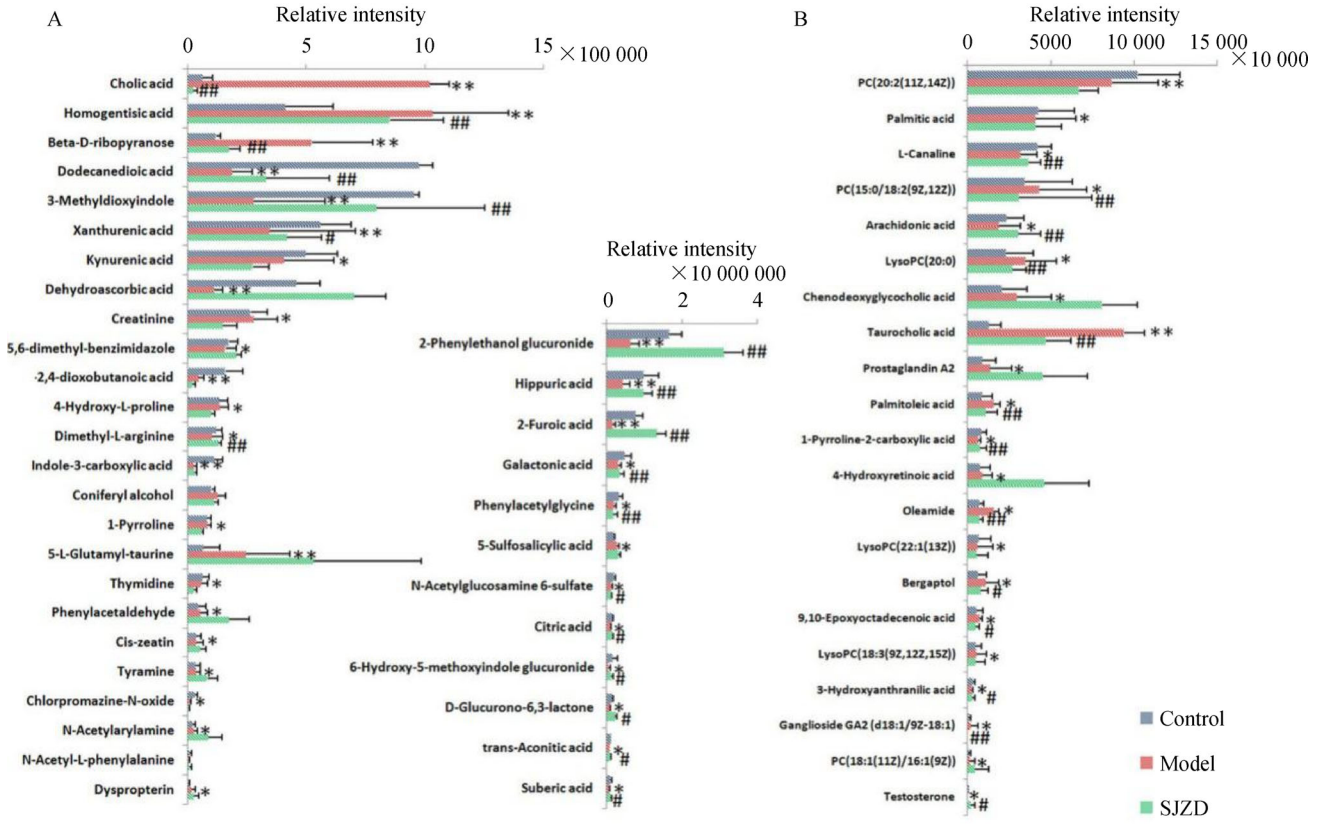

Fig. 5 Serum and urine biomarker relative measurements before and after SJZD treatment. (A) 37 urine metabolites. (B) 21 serum metabolites. (*$P < 0.05$ and **$P < 0.01$ compared with the control group; $^{\#}P < 0.05$ and $^{\#\#}P < 0.01$ compared with the model group.)

based on the compatibility principle of Chinese medicine and the first choice of "monarch drug in a prescription." We determined malonyl-ginsenoside Rb2 and ginsenoside Ro as the q-markers of ginseng; dehydrotumulosic acid and dihydroxy lanostene-triene-21-acid as the q-markers of poria; glycyrrhizic acid, isoglabrolide, and glycyrrhetnic acid as the q-markers of licorice; and 2-atractylenolide as the q-marker of macrocephala (Fig. 12).

Discussion

As an important part of TCM, the quality and safety of Chinese medicinal materials are the keys to promote the sustained and healthy development of Chinese medicine industry [31]. Meanwhile, when the QC standard of Chinese medicine is defective, the evaluation of the overall quality of the prescription decreases further. The evaluation on the basis of the presence or absence and increased or decreased amount of individual constituent indicator can hardly satisfy the evaluation need of TCM and cannot represent the complex herbal medicines. For example, ginseng is commonly evaluated by the ginsenoside Rg1 ($C_{42}H_{72}O_{14}$), ginsenoside Re ($C_{48}H_{82}O_{18}$), and ginsenoside Rb1 ($C_{54}H_{92}O_{23}$) contents. Meanwhile, the same genus *Panax* pseudo-ginseng possess the ginsenoside Rg1 ($C_{42}H_{72}O_{14}$) and ginsenoside Rb1 ($C_{54}H_{92}O_{23}$) as QC standards, and American ginseng shared all these standards. Such evaluation indicators are nonspecific, and the indicators used for evaluation may not necessarily represent the pharmaceutical effect of drugs. SJZD is composed of four kinds of Chinese medicines, only two of which have QC standards. The quality evaluation of macrocephala and poria were simply based on the control medicine, with no reliable components as the QC indexes. With regard to the clinically commonly used Sijunzi pills, the control medicinal materials were used to identify the pill, and the content of glycyrrhizin ($C_{42}H_{62}O_{16}$) was used as the quality standard. The other commonly used Sijunzi granules used the *Codonopsis*, *Poria*, *atractylodes*, and *Licorice* control medicines as the identification conditions. The glycyrrhizin ($C_{42}H_{62}O_{16}$) and liquiritin ($C_{21}H_{22}O_9$) contents are listed as the quality standards. The two Chinese patent medicines above have the same composition with the SJZD while they are evaluated by different standards. All QC standards lack specificity and are hardly

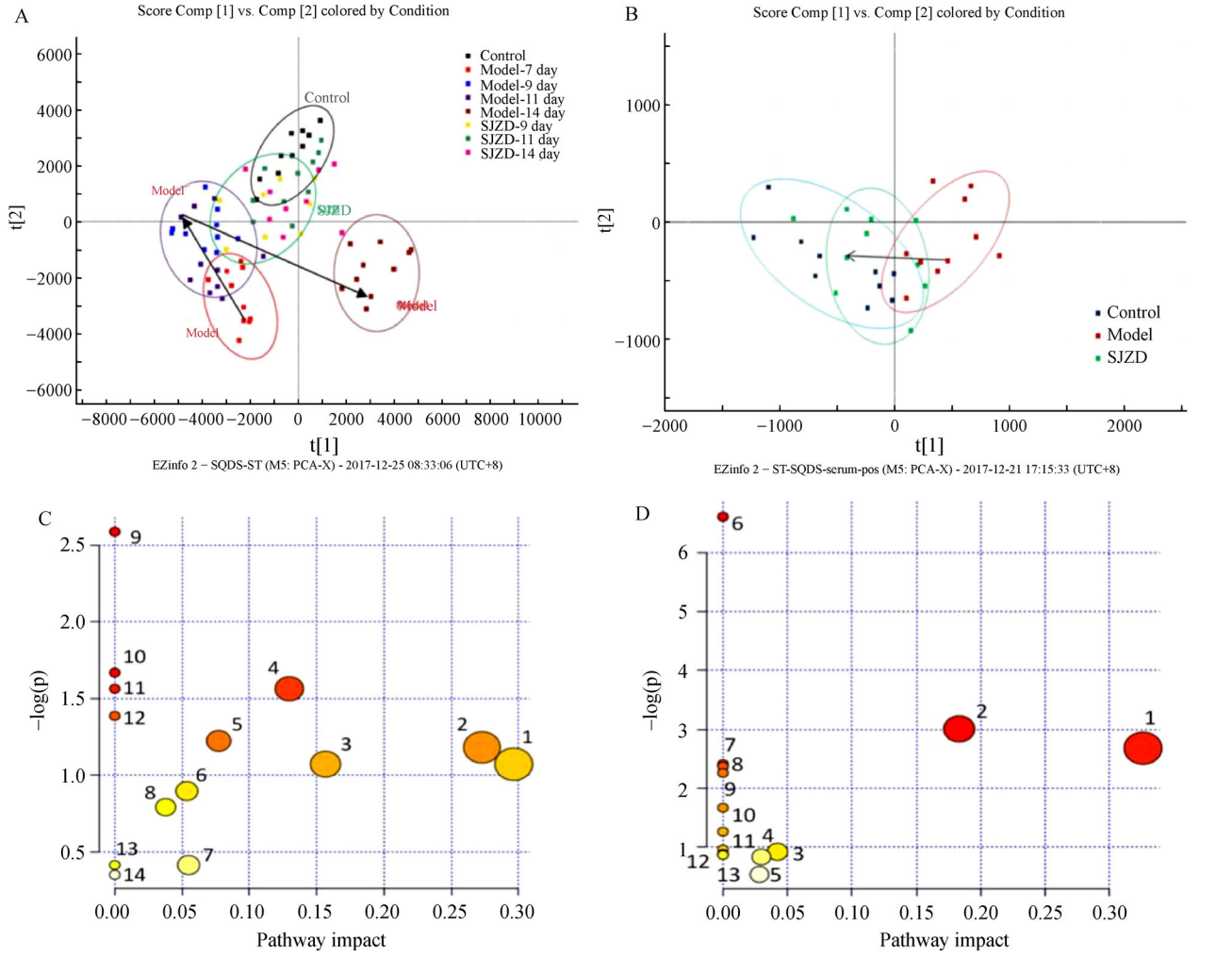

Fig. 6 Metabolite profile after orally administrated SJZD and the urine/serum metabolites relative-disordered pathway. (A) Urine metabolite profile. (B) Urine metabolite profile. (C) Urine metabolite relative pathways. 1. Glyoxylate and dicarboxylate metabolism; 2. Pentose and glucuronate interconversions; 3. Folate biosynthesis; 4. Phenylalanine metabolism; 5. Tyrosine metabolism; 6. Citrate cycle (TCA cycle); 7. Pyrimidine metabolism; 8. Starch and sucrose metabolism; 9. Ubiquinone and other terpenoid-quinone biosynthesis; 10. Taurine and hypotaurine metabolism; 11. Ascorbate and aldarate metabolism; 12. Riboflavin metabolism; 13. Tryptophan metabolism; 14. Primary bile acid biosynthesis. (D) Serum metabolite relative pathways. 1. Arachidonic acid metabolism; 2. Glycerophospholipid metabolism; 3. Tryptophan metabolism; 4. Primary bile acid biosynthesis; 5. Steroid hormone biosynthesis; 6. Linoleic acid metabolism; 7. Biosynthesis of unsaturated fatty acids; 8. Taurine and hypotaurine metabolism; 9. α-linolenic acid metabolism; 10. Retinol metabolism; 11. Fatty acid biosynthesis; 12. Arginine and proline metabolism; 13. Fatty acid elongation in the mitochondria.

reprehensive for the prescription efficacy. The above problems are very common in Chinese medicine QC, and specific q-markers, which can be representative for the efficacy of drugs, are urgent to be developed. We established and implemented a new Chinmedomics method to help control the quality of TCM. We also take SJZD as the research object in this pioneer experiment.

SJZD has the function of invigorating qi and strengthening the spleen. A common understanding in TCM and modern medicine is that a postnatal person's life process, and the production of the necessary nutrients all depend on the spleen. Notably, the spleen referred to in TCM includes the spleen and stomach in Western medicine. The stomach function is to accept food, the spleen function is to transport and transform the essence substances obtained from digestion, and the two are connected by meridians and collaterals to form an exterior–interior relationship, which constitutes the central link during dietary metabolism. Qi can promote and stimulate the physiologic function of the spleen, and the physiologic function of the spleen is the manifestation of the movement of spleen qi. When the spleen is full of qi, it plays normal physiologic function, transferring the transformed essence to the heart and lungs, offering essence and blood,

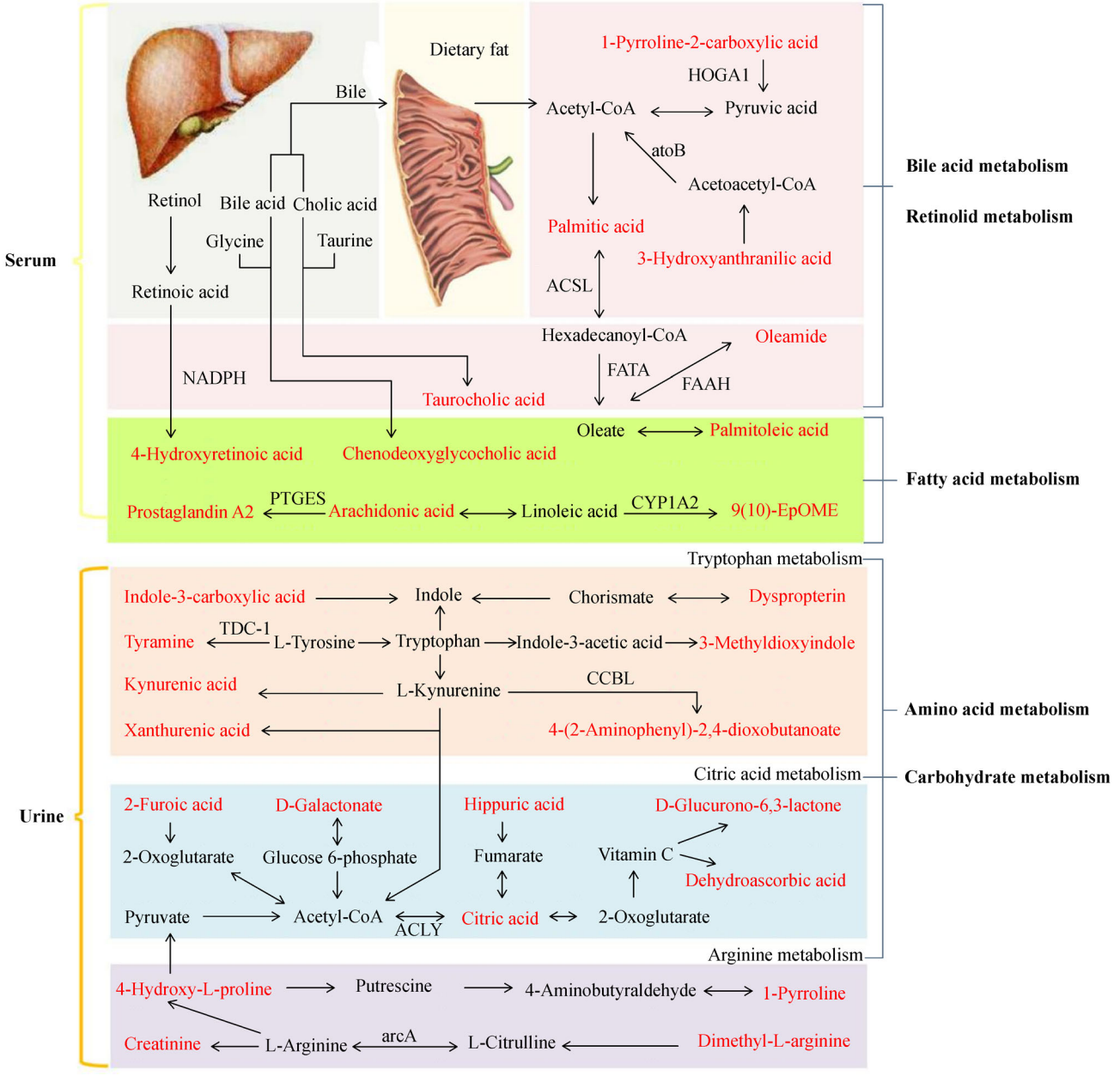

Fig. 7 Reconstructed pathways associated with the biomarkers that are abnormally expressed in SQDS rats. The red script substances are the metabolic markers tentatively identified in this experiment. They are mainly involved in bile acid metabolism, retinoid acid metabolism, fatty acid metabolism, amino acid metabolism, and carbohydrate metabolism.

spreading to the whole body. Thus, the *zang-fu*, meridians, limbs, tendons, and hair can be fully nourished and finally exert their normal physiologic functions. Conversely, if the spleen qi is weak, then it will lose its ability to transport and then affect the food digestion, weakening the absorption of essential substances and the distribution of the whole body. This condition leads to appetite loss, abdominal distention, loose stool, emaciation, and similar symptoms of anemia in clinical practice. In our current experiment, we replicated a symptomatic SQDS rat model by means of bitter cold and diarrhea-coupled disordered dietary; the general state, body weight, loose stool rate, and activity rate of the rats have been carefully recorded as they are the most direct symptoms corresponding to the diagnosis of SQDS in clinical practice [32,33]. Through further monitoring the serum biochemistry level, visceral index, and mucosal pathological manifestations, the SQDS rat model was confirmed in physiologically functional and

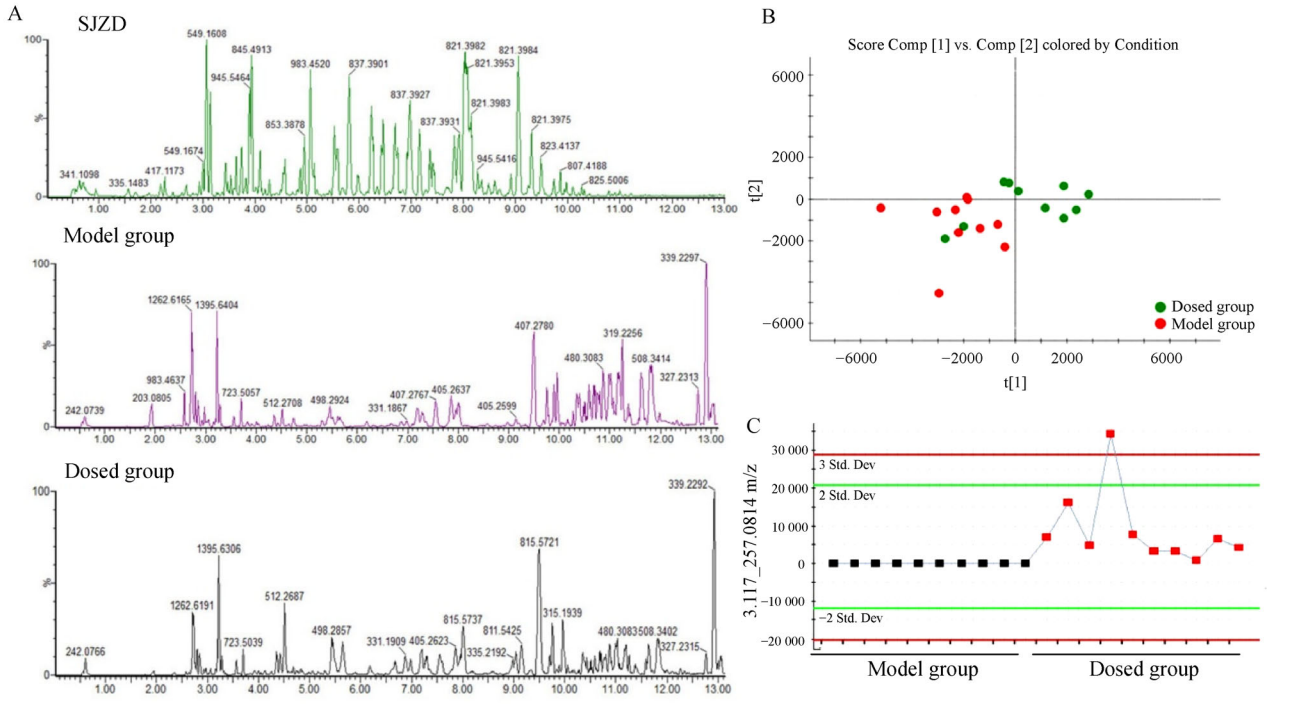

Fig. 8 Chromatograms and multivariate analysis in serum pharmacochemistry analysis. (A) Chromatograms of the SJZD, model group serum, and SJZD-dosed group. (B) PCA score plot between the dosed and model groups. (C) Trend plot of identified absorbed compound 3.117_257.0814.

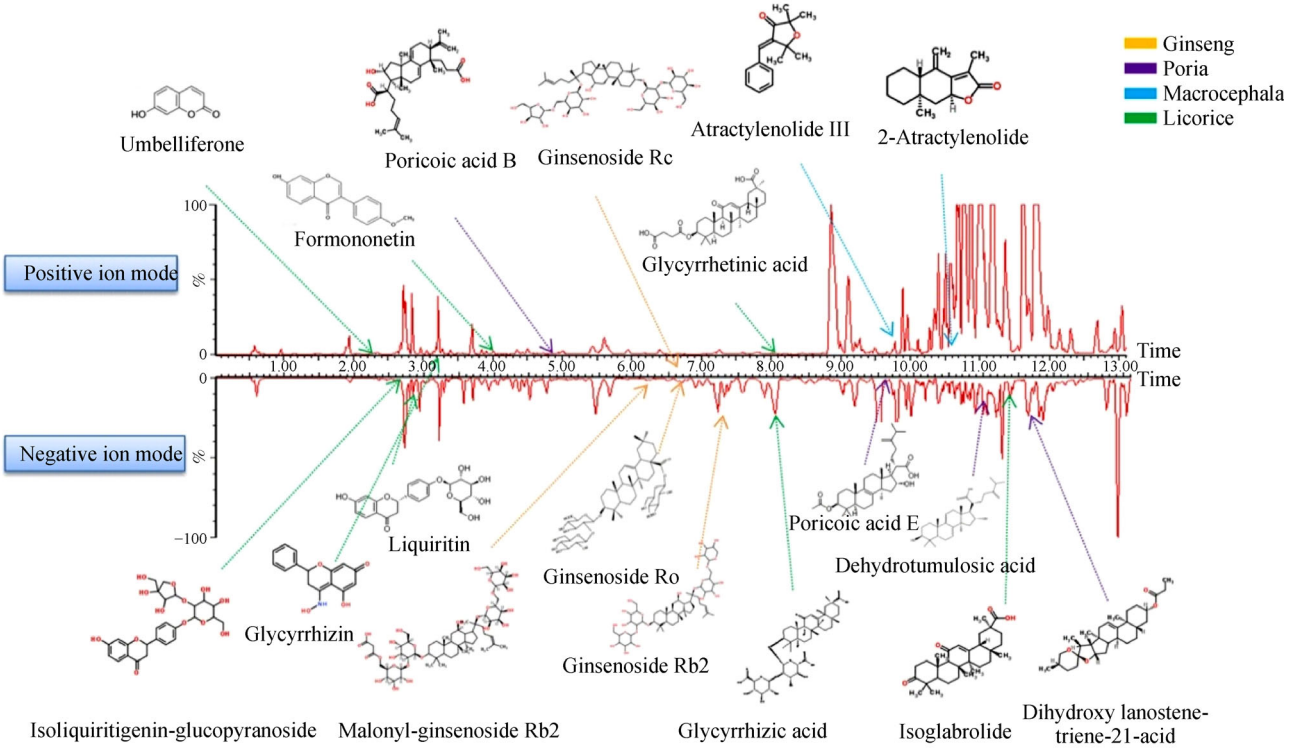

Fig. 9 ES-BPI rat serum chromatogram marked with characterized compounds after orally administrated SJZD. The compounds with yellow arrows were from Ginseng, with purple arrows from poria, with blue arrows from macrocephala, and with green arrows from licorice.

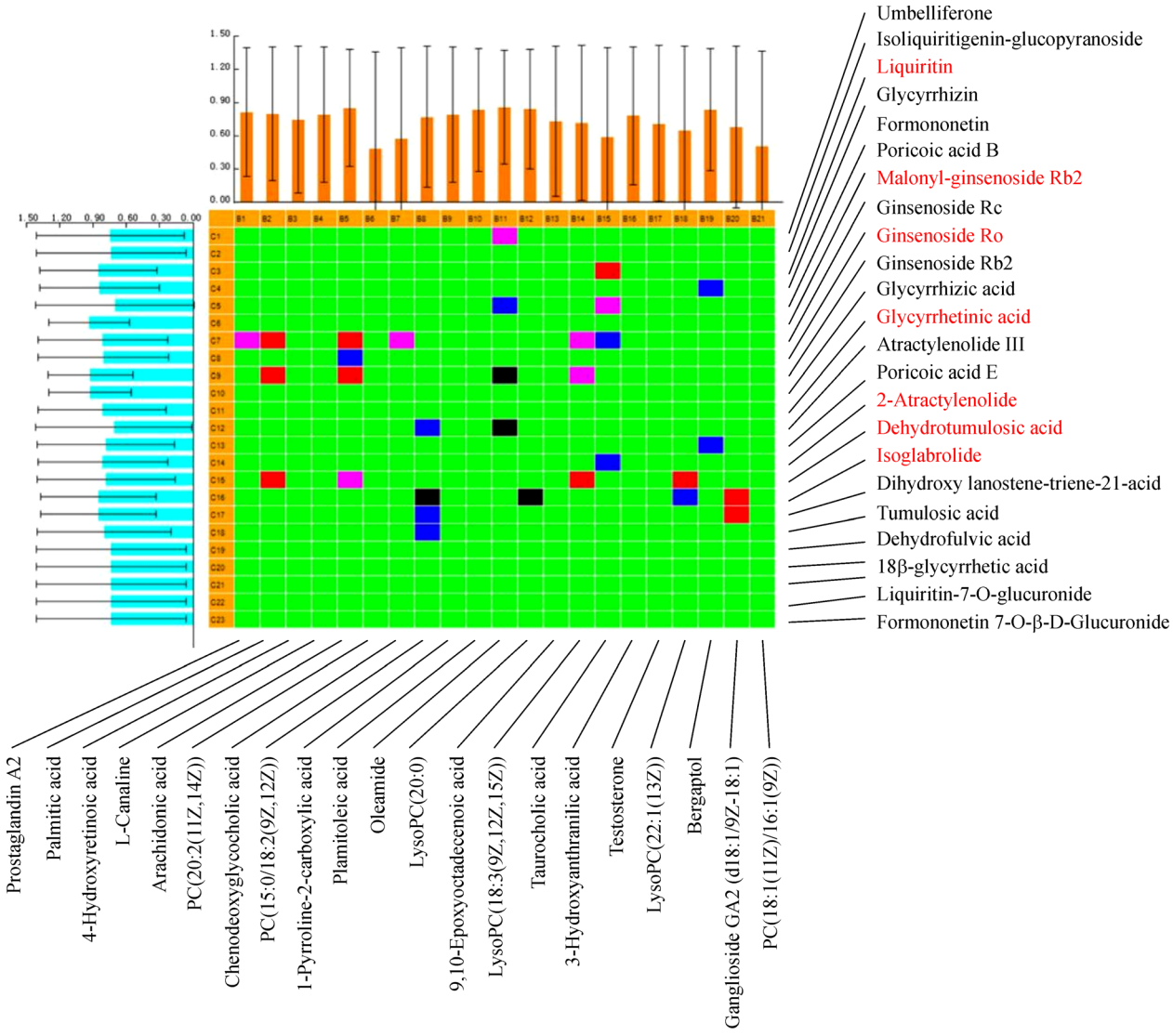

Fig. 10 PCMS analysis between serum biomarkers and chemical constituents in the SJZD group. The vertical arrangement is the absorption components, and the transverse arrangement is the biomarkers. Red square: means extremely positive correlation. Black square: means extremely negative correlation. Pink square: means highly positive correlation. Blue square: means highly negative correlation. Green square: means minimal correlation. The absorbed compounds marked in red were the crucial compounds, which we further screened.

morphology levels. We also clarified the efficacy of SJZD on SQDS with the same evaluation index, in which rats manifested improved physical condition after SJZD treatment.

The approach to use metabolomics for medicinal plants QC is not new [34]. Researchers have employed this strategy in the pharmacodynamic effects exploration, such as in *Citrus aurantium* L. pericarp, *Citrus aurantium* L. fruit [35], *Angelica sinensis* [36], Tufuling Granules [37], and *Phellinus igniarius* [38]. The TCM therapeutic potentials were extensively elaborated [39,40], with the TCM toxicity objective evaluation even realized [41]. Here, with the purpose of interpreting the SJZD efficacy, we duplicated the TCM syndrome model corresponding to the decoction and utilized the metabolomics for the representative substance excavation on the level of metabolites, and the markers found under the TCM syndrome state can be regarded as its characteristics to some extent [42]. In the serum and urine metabonomic study of rats with SQDS, we found that metabolites with disordered expression levels were mainly in the bile acid metabolism, retinoid acid metabolism, amino acid metabolism, fatty acid metabolism, and carbohydrate metabolism. Bile acid is an important component of bile, playing an important role in maintaining the balance of fat metabolism. In our experiment, we found that taurocholic

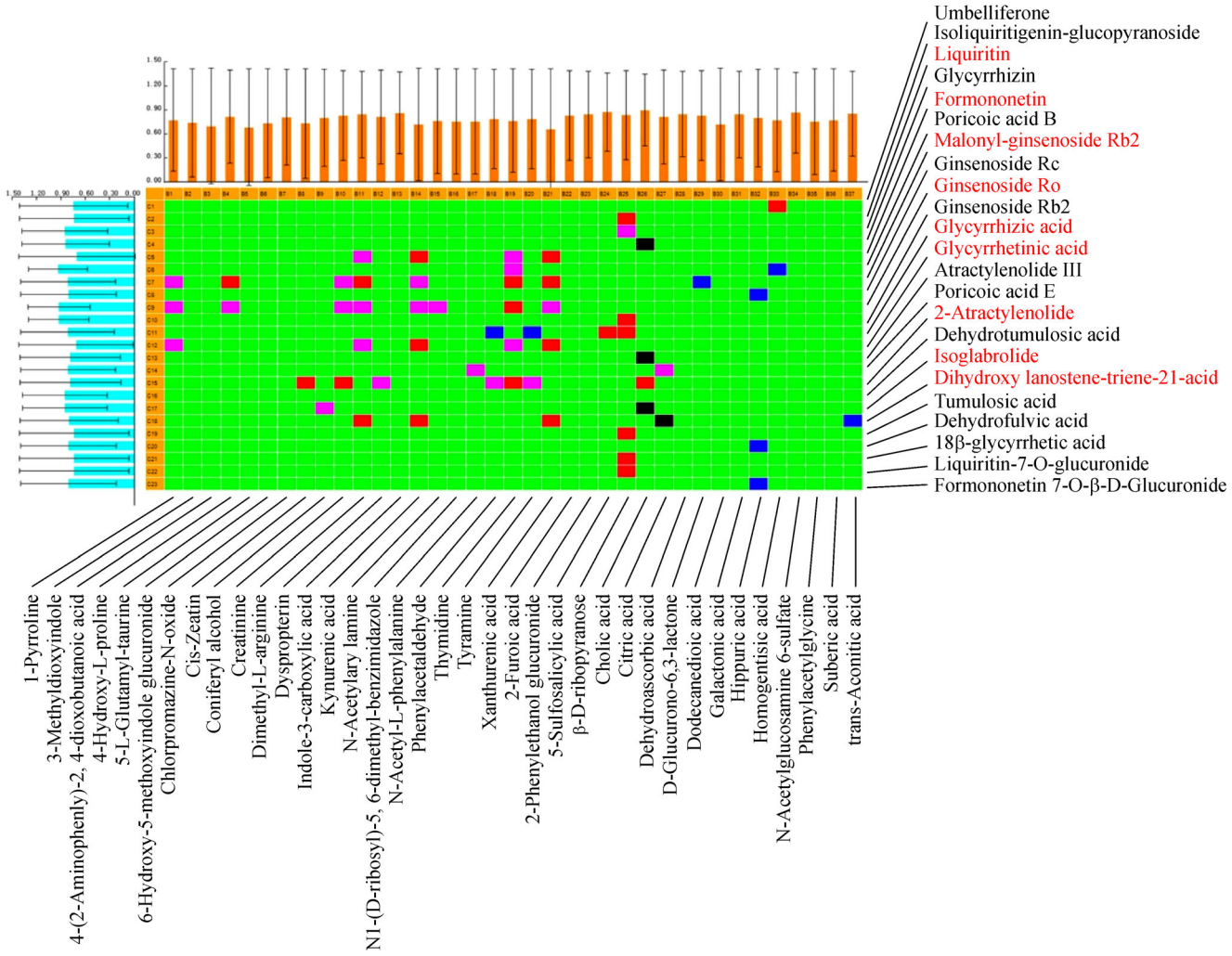

Fig. 11 PCMS analysis between urine biomarkers and chemical constituents in the SJZD group. The vertical arrangement is the absorption components, and the transverse arrangement is the biomarkers. Red square: means extremely positive correlation. Black square: means extremely negative correlation. Pink square: means highly positive correlation. Blue square: means highly negative correlation. Green square: means minimal correlation. The absorbed compounds marked in red were the crucial compounds, which we further screened.

acid and chenodeoxyglycocholic acid were disordered expressed, and they are essential for the absorption of dietary fats and vitamins [43]. In addition, taurocholic acid lays the key position at the junction of the primary bile acids and secondary bile acid biosynthesis processes. The 4-hydroxyretinoic acid is abnormally expressed metabolites involved in retinoid acid metabolism among the current experiment. Retinoid acid plays a crucial role in supporting the systemic function of vitamin A *in vitro* [44] and also influences the normal immune function [45]. From the results of the organ indexes, we speculated that some degree of decline may exist in immunity in the model rats. This finding may have some relations with the disordered expression of retinoid acid metabolism. Abnormally expressed 4-hydroxy-L-proline, 5-L-glutamyl-taurine, 5-sulfosalicylic acid, 6-hydroxy-5-methoxyindole glucuronide, β-D-ribopyranose, and chlorpromazine-N-oxide are metabolites belonging to the sub-class of amino acid, peptides, and analogs according to the search results in the Human Metabolome database. Under normal circumstances, amino acids are obtained through food digestion and absorption, tissue protein decomposition, body synthesis, and further decomposed by enzymes through deamination and decarboxylation. Amino acids in the human body should be in a state of dynamic balance and convert sugar and fat during the balanced process of amino acid and then excreted into urea, carbon dioxide, and water. Fatty acid metabolism and carbohydrate metabolism are important components of the body's energy metabolism. In the current experiment, we found that metabolites, such as palmitoleic acid, arachidonic acid, 9,10-epoxyoctadecenoic acid, and D-glucurono-6,3-

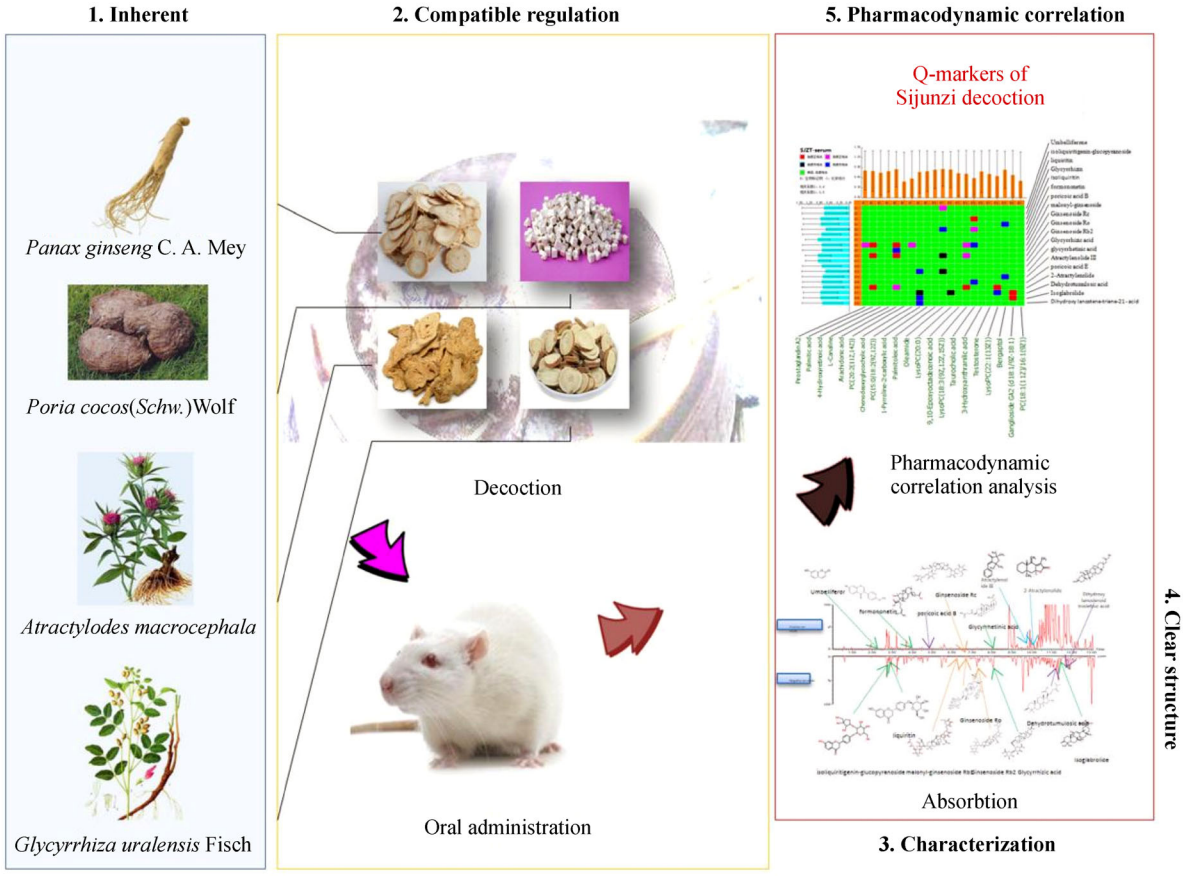

Fig. 12 Research route of Sijunzi decoction's quality-marker in this experiment.

lactone, were disordered expressed. Fatty acid metabolism is a process in which the body breaks down fatty acids, making diets an intermediate part of the available ingredients with the biological function building new proteins and storing energy. Carbohydrate is the main component of life cell structure and the main energy-supplying substance and has the important function of regulating cell activity. In this study, the ability of the spleen to transform food and produce essential substances was weakened in the model rats due to spleen qi deficiency. This result also corresponded to the disorder markers, which we found from the standpoint of metabonomics. We characterized the metabolic profiles of the SQDS rats and observed the callback function of SJZD, partial of the above abnormal performance improvements or indicator callbacks offering the possibility to ensure the q-markers under the SJZD effectiveness.

According to the theory and method of serum pharmacochemistry [46], through certain transmission routes, drugs enter blood, metabolize, distribute, and produce specific biological effects. The blood components are the final "effect components." We characterized 23 final effective components of SJZD *in vitro* and preliminarily identified 10 substances, highly correlated with the drug efficacy. The 10 substances originate from all compatibility medicines, indicating that under the four Chinese medicine combination circumstance, the prescriptions can fulfill the treatment purpose. Through further screening, we finally determined eight q-markers for SJZD, and these substances are all prototype component absorbed into the serum with high correlation between the QC indices of TCMs and the effectiveness. As the sovereign drug, ginseng has the efficacy of tonifying qi. In addition, the highly correlated compounds malonyl-ginsenoside Rb2 and ginsenoside Ro, which we found in our experiment, could be representative tonifying qi function of ginseng. Considering the perspective of mass transfer and traceability, the effective components in the blood are the final link of the mass transfer system. We have many reasons to regard the SJZD effective compounds in our SQDS model rat becoming the q-markers of ginseng in the prescription. Similarly, the q-markers of dehydrotumulosic acid and dihydroxy lanostene-triene-21-acid reflected the function of poria, and glycyrrhizic acid,

isoglabrolide, and glycyrrhetnic acid reflected the function of licorice. Meanwhile, 2-atractylenolide reflected the macrocephala function. The results obtained through the combination of the serum direct acting substances and the syndromes in the body represent the efficacy of the medicine and reflect the essence of the prescription-TCM syndrome. This finding clearly exhibited the characteristics of the treatment of disease in TCM.

Metabolomics plays an important role in exploring the metabolic disorder metabolism-related diseases [47–55], biomarker identification [56–61], and response to treatment [62–68]. The concepts of holistic approach, syndrome differentiation, and yin-yang concept are the quintessence of TCM theoretical science. They are in line with metabolomics approach but need to be transformed and modernized into upgraded TCM theory by using worldwide commonly accepted scientific terms and theories. The Chinmedomics method we proposed in this study integrates the metabolomics and serum pharmacochemistry methods supported by modern technology and visualizes the syndromes of TCM and the effects of prescriptions, characterizes the modern biological essence of Traditional Chinese Medicine SQDS at the metabolite level, and discovers the key components of prescriptions in the syndrome treatment. Our foundation advanced the specificity of QC of SJZD and made the connection between the quality attribute and the complex system of TCM come true. The most important thing is that using such a marker to evaluate the medicine quality can avoid the problem of repeated use of the same index in different Chinese medicine evaluation. The q-markers found in the prescription also realizes the purpose of combining the quality standard of different drugs with the corresponding prescription effect.

Conclusions

The safety, effectiveness, and controllability of Chinese herbal pieces are the basic requirements in clinical practice. The pharmacopoeia standard is the basic guarantee for the QC of decoction pieces. To improve the quality standard of TCM further, we replicated in this experiment the rat model corresponding to the SJZD, determined the therapeutic effect of SJZD, and found the components absorbed into the blood on the SJZD rat. Finally, we adopted the Chinmedomics method to correlate the compounds with the metabolic biomarkers. On the basis of this condition, the pharmacodynamic material bases related to therapeutic effects were identified, and further screening was carried out under the guidance of q-marker principle. This work is the first to report the prescription q-markers, which exist in traceable medicinal materials under the precondition of effectiveness and compatibility. Deficiencies were still observed in the study of TCM in modern society. TCM theory emphasized the macroscopic characteristics and showed the relationship among various parts. This theory often expounds the internal laws of the human body by means of "extrapolating from the outside to the inside" and "taking substances with similar properties as a class" while only seeing the macroscopic appearance. However, TCM neglects the microscopic features or only pays attention to fuzzy overall outline but lacks partial detail description, thereby often giving specious ambiguity conclusion. Similarly, Western medicine pays excessive attention to local details (target organs and target tissue lesions) and neglects the whole; thus, a partial error can be easily made. Thus, constructing a modern research method system that conforms to the characteristics of TCM is extremely important. At present, the phenomena of "prescription – disease – syndrome" splitting and "gene – protein – metabolite" separating are common in the study of modernization of TCM. Under the guidance of Chinmedomics theories, we hope that we can break the deadlock of splitting the current study of TCM. Thus, the study of TCM syndrome is indeed related to the corresponding prescriptions. Although Chinmedomics is a good method, careful research is still needed to improve the correlation between prescriptions and syndromes.

Acknowledgements

This work was supported by grants from the National Key Research and Development Program of China (No. 2018YFC1706103), Key Program of National Natural Science Foundation of China (Nos. 81830110, 8181101160, 81430093, 81673586, 81703685, 81302-905, 81503386, and 81373930), National Key Subject of Drug Innovation (Nos. 2015ZX09101043-005 and 2015ZX09101043-011), TCM State Administration Subject of Public Welfare of (No. 2015468004), Major Projects of Application Technology Research and Development Plan in Heilongjiang Province (No. GX16C003), TCM State Administration Subject of Public Welfare (No. 2015468004), Young Talent Lift Engineering Project of China Association of Traditional Chinese Medicine (No. QNRC2-B06), and Outstanding Talents Foundation of Heilongjiang University of Chinese Medicine (No. 2018jc01).

Compliance with ethics guidelines

Qiqi Zhao, Xin Gao, Guangli Yan, Aihua Zhang, Hui Sun, Ying Han, Wenxiu Li, Liang Liu, and Xijun Wang declared no conflicts of interest. All institutional and national guidelines for the care and use of laboratory animals were followed. Approval for the animal experimental studies was received from the Institutional Animal Care and Use Committees of Heilongjiang University of Chinese Medicine.

Electronic Supplementary Material Supplementary material is available in the online version of this article at https://doi.org/10.1007/s11684-019-0705-9 and is accessible for authorized users.

References

1. Hu J, Liu B. The basic theory, diagnostic, and therapeutic system of traditional Chinese medicine and the challenges they bring to statistics. Stat Med 2012; 31(7): 602–605
2. Liu X, Fu J, Fan T, Liu W, Jiang H, Zhang R, Ding H, Yang H, Hu S, Huang Y, Li G, Lan Y, She B, Mao B. The efficacy and safety of Shen Guo Lao Nian Granule for common cold of qi-deficiency syndrome: study protocol for a randomized, double-blind, placebo-controlled, multicenter, phase II clinical trial. Evid Based Complement Alternat Med 2017; 2017(6): 1806461
3. Shu Q, Sun D, Wang H, Liang F, Gerhard L, Daniela L, Ingrid G, Chen L, He W, Wang Y. Differences of acupuncture and moxibustion on heart rate variability in *qi*-deficiency syndrome:a randomized controlled trial. Chin Acup Moxib (Zhongguo Zhen Jiu) 2017; 37(1): 25–30 (in Chinese)
4. Xu D, Shen Z, Wang W. Immunoregulation of Youguiyin, Sijunzitang, Taohong Siwutang in treating patients with deficiency of kidney, spleen and blood stasis syndrome. Chin J Integr Trad West Med (Zhongguo Zhong Xi Yi Jie He Za Zhi) 1999; 19(12): 712–714 (in Chinese)
5. Hu Q, Calduch RM. On traditional Chinese medicine regulation in China: how quality and safety of use are insured. Pharmacol Res 2017; 119: 371–372
6. Wang G, Mao B, Xiong ZY, Fan T, Chen XD, Wang L, Liu GJ, Liu J, Guo J, Chang J, Wu TX, Li TQ; CONSORT Group for Traditional Chinese Medicine. The quality of reporting of randomized controlled trials of traditional Chinese medicine: a survey of 13 randomly selected journals from mainland China. Clin Ther 2007; 29(7): 1456–1467
7. Ning Z, Lu C, Zhang Y, Zhao S, Liu B, Xu X, Liu Y. Application of plant metabonomics in quality assessment for large-scale production of traditional Chinese medicine. Planta Med 2013; 79(11): 897–908
8. Cheng TF, Jia YR, Zuo Z, Dong X, Zhou P, Li P, Li F. Quality assessment of traditional Chinese medicine herb couple by high-performance liquid chromatography and mass spectrometry combined with Chemometrics. J Sep Sci 2016; 39(7): 1223–1231
9. Wang C, Hu S, Chen X, Bai X. Screening and quantification of anticancer compounds in traditional Chinese medicine by hollow fiber cell fishing and hollow fiber liquid/solid-phase microextraction. J Sep Sci 2016; 39(10): 1814–1824
10. Zhuo L, Peng J, Zhao Y, Li D, Xie X, Tong L, Yu Z. Screening bioactive quality control markers of QiShenYiQi dripping pills based on the relationship between the ultra-high performance liquid chromatography fingerprint and vascular protective activity. J Sep Sci 2017; 40(20): 4076–4084
11. Wang X, Zhang A, Sun H, Yan G. Precision diagnosis of Chinese medicine syndrome and evaluation of prescription efficacy based on Chinmedomics. Modernization Tradit Chin Med Materia Medica—World Sci Technol (Shi Jie Ke Xue Ji Shu— Zhong Yi Yao Xian Dai Hua) 2017; 19(1): 30–34 (in Chinese)
12. Zhang A, Sun H, Yan G, Wang P, Han Y, Wang XJ. Chinmedomics: a new strategy for research of traditional Chinese medicine. China J Chin Materia Medica (Zhongguo Zhong Yao Za Zhi) 2015; 40(4): 569–576 (in Chinese)
13. Wang H, Shi S, Wang S. Can highly cited herbs in ancient traditional Chinese medicine formulas and modern publications predict therapeutic targets for diabetes mellitus? J Ethnopharmacol 2018; 213: 101–110
14. Wang X, Zhang A, Sun H. Future perspectives of Chinese medical formulae: Chinmedomics as an effector. OMICS 2012; 16(7-8): 414–421
15. Wang X, Zhang A, Hui S, Han Y, Yan G. Discovery and development of innovative drug from traditional medicine by integrated Chinmedomics strategies in the post-genomic era. Trends Analyt Chem 2016; 76: 86–94
16. Li XN, Zhang A, Wang M, Sun H, Liu Z, Qiu S, Zhang T, Wang X. Screening the active compounds of *Phellodendri amurensis* cortex for treating prostate cancer by high-throughput Chinmedomics. Sci Rep 2017; 7(1): 46234
17. Zhou XH, Zhang AH, Wang L, Tan YL, Guan Y, Han Y, Sun H, Wang XJ. Novel Chinmedomics strategy for discovering effective constituents from ShenQiWan acting on ShenYangXu syndrome. Chin J Nat Med 2016; 14(8): 561–581
18. Wang X, Zhang A, Zhou X, Liu Q, Nan Y, Guan Y, Kong L, Han Y, Sun H, Yan G. An integrated Chinmedomics strategy for discovery of effective constituents from traditional herbal medicine. Sci Rep 2016; 6(1): 18997
19. Liu F, Liu Y, Tian C. Effect of Rhizoma Atractylodis extract in protecting gastric mucosa and modulating gastrointestinal immune function in a rat model of spleen deficiency. J Southern Med Univ (Nan Fang Yi Ke Da Xue Xue Bao) 2015; 35(3): 343–347, 354 (in Chinese)
20. Lu S, Han Y, Chu H, Kong L, Zhang A, Yan G, Sun H, Wang P, Wang X. Characterizing serum metabolic alterations of Alzheimer's disease and intervention of Shengmai-San by ultra-performance liquid chromatography/electrospray ionization quadruple time-of-flight mass spectrometry. Food Funct 2017; 8(4): 1660–1671
21. Zhao Q, Zhang A, Zong W, An N, Zhang H, Luan Y, Sun H, Wang X, Cao H. Exploring potential biomarkers and determining the metabolic mechanism of type 2 diabetes mellitus using liquid chromatography coupled to high-resolution mass spectrometry. RSC Adv 2017; 7(70): 44186–44198
22. de Passillé AM, Pelletier G, Ménard J, Morisset J. Relationships of weight gain and behavior to digestive organ weight and enzyme activities in piglets. J Anim Sci 1989; 67(11): 2921–2929
23. Tharakan A, Norton IT, Fryer PJ, Bakalis S. Mass transfer and nutrient absorption in a simulated model of small intestine. J Food Sci 2010; 75(6): E339–E346
24. Clara R, Schumacher M, Ramachandran D, Fedele S, Krieger JP, Langhans W, Mansouri A. Metabolic adaptation of the small intestine to short- and medium-term high-fat diet exposure. J Cell Physiol 2017; 232(1): 167–175
25. Mansi C, Borro P, Giacomini M, Biagini R, Mele MR, Pandolfo N, Savarino V. Comparative effects of levosulpiride and cisapride on gastric emptying and symptoms in patients with functional dyspepsia and gastroparesis. Aliment Pharmacol Ther 2000; 14 (5): 561–569
26. Tortora GJ, Anagnostakos NP. Principles of anatomy and physiology. J Anat 2009; 86(10): 555
27. Zhang SY, Peng GY, Gu LG, Li ZM, Yin SJ. Effect and mechanisms of Gong-tone music on the immunological function in rats with Liver (Gan)-qi depression and Spleen (Pi)-qi deficiency syndrome in rats. Chin J Integr Med 2013; 19(3): 212–216

28. Itoh Z, Takeuchi S, Aizawa I, Mori K, Taminato T, Seino Y, Imura H, Yanaihara N. Changes in plasma motilin concentration and gastrointestinal contractile activity in conscious dogs. Am J Dig Dis 1978; 23(10): 929–935
29. Liu Q, Cai G. Content of somatostatin and cholecystokinin-8 in hypothalamus and colons in a rat model of spleen-deficiency syndrome. J Chin Integr Med (Zhong Xi Yi Jie He Xue Bao) 2007; 5 (5): 555–558 (in Chinese)
30. Yong RL, Qu Y, Li XX, Wang JB, Xue YN, Zhang LD. Effect of electroacupuncture at "Zusanli"(ST 36) on the expression of Ghrelin/cAMP/PKA in the Jejunum in rats with spleen *Qi* deficiency syndrome. Acupunct Res (Zhen Ci Yan Jiu) 2016; 41(6): 497–501 (in Chinese)
31. Chan K, Leung K, Lu G. Quality and safety should go hand in hand to monitor herbal products: examples from Chinese medicinal materials (CMM). Planta Med 2007; 73(9): 803
32. Duan YQ, Cheng YX, Liang YJ, Cheng WD, Du J, Yang XY, Wang Y. Intervention of qi-activating and spleen-strengthening herbs on Ca^{2+}/CaMK II signaling pathways key factors in skeletal muscle tissue of rats with spleen-qi deficiency. J Chin Med Mater (Zhong Yao Cai) 2015; 38(3): 562–566 (in Chinese)
33. Zheng XF, Tian JS, Liu P, Xing J, Qin XM. Analysis of the restorative effect of *Bu-zhong-yi-qi-tang* in the spleen-qi deficiency rat model using ^{1}H-NMR-based metabonomics. J Ethnopharmacol 2014; 151(2): 912–920
34. Sun H, Zhang AH, Yang L, Li MX, Fang H, Xie J, Wang XJ. High-throughput chinmedomics strategy for discovering the quality-markers and potential targets for Yinchenhao decoction. Phytomedicine 2019; 54: 328–338
35. Zhao S, Liu Z, Wang M, He D, Liu L, Shu Y, Song Z, Li H, Liu Y, Lu A. Anti-inflammatory effects of Zhishi and Zhiqiao revealed by network pharmacology integrated with molecular mechanism and metabolomics studies. Phytomedicine 2018; 50: 61–72
36. Yuan Z, Zhong L, Hua Y, Ji P, Yao W, Ma Q, Zhang X, Wen Y, Yang L, Wei Y. Metabolomics study on promoting blood circulation and ameliorating blood stasis: investigating the mechanism of *Angelica sinensis* and its processed products. Biomed Chromatogr 2019; 33(4): e4457
37. Wu P, Li J, Zhang X, Zeng F, Liu Y, Sun W. Study of the treatment effects of compound Tufuling Granules in hyperuricemic rats using serum metabolomics. Evid Based Complement Alternat Med 2018; 2018: 3458185
38. Dong Y, Qiu P, Zhao L, Zhang P, Huang X, Li C, Chai K, Shou D. Metabolomics study of the hepatoprotective effect of *Phellinus igniarius* in chronic ethanol-induced liver injury mice using UPLC-Q/TOF-MS combined with ingenuity pathway analysis. Phytomedicine2018 Oct 2. 152697
39. Tripathi N, Shrivastava D, Ahmad Mir B, Kumar S, Govil S, Vahedi M, Bisen PS. Metabolomic and biotechnological approaches to determine therapeutic potential of *Withania somnifera* (L.) Dunal: a review. Phytomedicine 2018; 50: 127–136
40. Xu Y, Chen S, Yu T, Qiao J, Sun G. High-throughput metabolomics investigates anti-osteoporosis activity of oleanolic acid via regulating metabolic networks using ultra-performance liquid chromatography coupled with mass spectrometry. Phytomedicine 2018; 51: 68–76
41. Duan L, Guo L, Wang L, Yin Q, Zhang CM, Zheng YG, Liu EH. Application of metabolomics in toxicity evaluation of traditional Chinese medicines. Chin Med 2018; 13(1): 60
42. Wang X, Zhang S, Zhang A, Yan G, Wu X, Han Y, Sun H. Metabolomics study of type 2 diabetes and therapeutic effects of Tianqijiangtang-capsule using ultra-performance liquid chromatography/electrospray ionization quadruple time-of-flight mass spectrometry. Anal Methods 2013; 5(9): 2218–2226
43. Zhang Y, Klaassen CD. Effects of feeding bile acids and a bile acid sequestrant on hepatic bile acid composition in mice. J Lipid Res 2010; 51(11): 3230–3242
44. Roberts AB, Frolik CA, Nichols MD, Sporn MB. Retinoid-dependent induction of the *in vivo* and *in vitro* metabolism of retinoic acid in tissues of the vitamin A-deficient hamster. J Biol Chem 1979; 254(14): 6303–6309
45. Hall JA, Grainger JR, Spencer SP, Belkaid Y. The role of retinoic acid in tolerance and immunity. Immunity 2011; 35(1): 13–22
46. Wang XJ. Progress and future developing of the serum pharmacochemistry of traditional Chinese medicine. China J Chin Mater Med (Zhongguo Zhong Yao Za Zhi) 2006; 31(10): 789–792, 835 (in Chinese)
47. Zhang AH, Yu JB, Sun H, Kong L, Wang XQ, Zhang QY, Wang XJ. Identifying quality-markers from Shengmai San protects against transgenic mouse model of Alzheimer's disease using Chinmedomics approach. Phytomedicine 2018; 45: 84–92
48. Sun H, Zhang AH, Song Q, Fang H, Liu XY, Su J, Yang L, Yu MD, Wang XJ. Functional metabolomics discover pentose and glucuronate interconversion pathways as promising targets for Yang Huang syndrome treatment with Yinchenhao Tang. RSC Adv 2018; 8(64): 36831–36839
49. Zhang AH, Sun H, Yan GL, Zhao QQ, Wang XJ. Chinmedomics: a powerful approach integrating metabolomics with serum pharmacochemistry to evaluate the efficacy of traditional Chinese medicine. Engineering (Beijing) 2019; 5(1): 60–68
50. Wang XJ, Lv HT, Zhang AH, Sun WJ, Liu L, Wang P, Wu ZM, Zou DX, Sun H. Metabolite profiling and pathway analysis of acute hepatitis rats by UPLC-ESI MS combined with pattern recognition methods. Liver Int 2014; 34(5): 759–770
51. Zhang AH, Sun H, Xu HY, Qiu S, Wang XJ. Cell metabolomics. OMICS 2013; 17(10): 495–501
52. Sun H, Zhang AH, Liu SB, Qiu S, Li XN, Zhang TL, Liu L, Wang XJ. Cell metabolomics identify regulatory pathways and targets of magnoline against prostate cancer. J Chromatogr B Analyt Technol Biomed Life Sci 2018; 1102–1103: 143–151
53. Zhang AH, Sun H, Wang XJ. Urinary metabolic profiling of rat models revealed protective function of scoparone against alcohol induced hepatotoxicity. Sci Rep 2015; 4(1): 6768
54. Liu XY, Zhang AH, Fang H, Li MX, Song Q, Su J, Yu MD, Yang L, Wang XJ. Serum metabolomics strategy for understanding the therapeutic effects of Yin-Chen-Hao-Tang against Yanghuang syndrome. RSC Adv 2018; 8(14): 7403–7413
55. Zhang AH, Sun H, Yan GL, Yuan Y, Han Y, Wang XJ. Metabolomics study of type 2 diabetes using ultra-performance LC-ESI/quadrupole-TOF high-definition MS coupled with pattern recognition methods. J Physiol Biochem 2014; 70(1): 117–128
56. Song Q, Zhang AH, Yan GL, Liu L, Wang XJ. Technological advances in current metabolomics and its application in tradition Chinese medicine. RSC Adv 2017; 7(84): 53516–53524

57. Zhang AH, Sun H, Sun WJ, Wang XJ. Metabolomics and Proteomics Annotate Therapeutic Mechanisms of Geniposide[M]// Chinmedomics. Amsterdam: Academic Press, 2015: 157–173
58. Zhao QQ, Zhang AH, Zong WJ, An N, Zhang HM, Luan YH, Cao HX, Sun H, Wang XJ. Chemometrics strategy coupled with high resolution mass spectrometry for analyzing and interpreting comprehensive metabolomic characterization of hyperlipemia. RSC Adv 2016; 6(113): 112534–112543
59. Wang XJ, Han Y, Zhang AH, Sun H. Metabolic profiling provides a system for the understanding of Alzheimer's disease in rats post-treatment with Kaixin San[M]//Chinmedomics. Amsterdam: Academic Press, 2015: 347–362
60. Zhang AH, Wang HY, Sun H, Zhang Y, An N, Yan GL, Meng XC, Wang XJ. Metabolomics strategy reveals therapeutical assessment of limonin on nonbacterial prostatitis. Food Funct 2015; 6(11): 3540–3549
61. Ren JL, Zhang AH, Kong L, Wang XJ. Advances in mass spectrometry-based metabolomics for investigation of metabolites. RSC Adv 2018; 8(40): 22335–22350
62. Zhang AH, Sun H, Wang XJ. Mass spectrometry-driven drug discovery for development of herbal medicine. Mass Spectrom Rev 2018; 37(3): 307–320
63. Sun H, Wang M, Zhang AH, Ni B, Dong H, Wang XJ. UPLC-Q-TOF-HDMS analysis of constituents in the root of two kinds of Aconitum using a metabolomics approach. Phytochem Anal 2013; 24(3): 263–276
64. Wu FF, Sun H, Wei WF, Han Y, Wang P, Dong TW, Yan GL, Wang XJ. Rapid and global detection and characterization of the constituents in ShengMai San by ultra-performance liquid chromatography-high-definition mass spectrometry. J Sep Sci 2011; 34(22): 3194–3199
65. Wang XJ, Zhang AH, Sun H, Han Y, Yan GL. Discovery and development of innovative drug from traditional medicine by integrated Chinmedomics strategies in the post-genomic era. TrAC Trends in Analytical Chemistry 2016; 76: 86–94
66. Zhang AH, Sun H, Qiu S, Wang XJ. Advancing drug discovery and development from active constituents of Yinchenhao Tang, a famous traditional Chinese medicine formula. Evid Based Complement Alternat Med 2013; 2013: 257909
67. Wang XJ, Wang QQ, Zhang AH, Zhang FM, Zhang H, Sun H, Cao HX, Zhang HM. Metabolomics study of intervention effects of Wen-Xin-Formula using ultra high-performance liquid chromatography/mass spectrometry coupled with pattern recognition approach. J Pharm Biomed Anal 2013; 74: 22–30
68. Dong W, Wang P, Meng XC, Sun H, Zhang AH, Wang WM, Dong H, Wang XJ. Ultra-performance liquid chromatography-high-definition mass spectrometry analysis of constituents in the root of Radix Stemonae and those absorbed in blood after oral administration of the extract of the crude drug. Phytochem Anal 2012; 23(6): 657–667